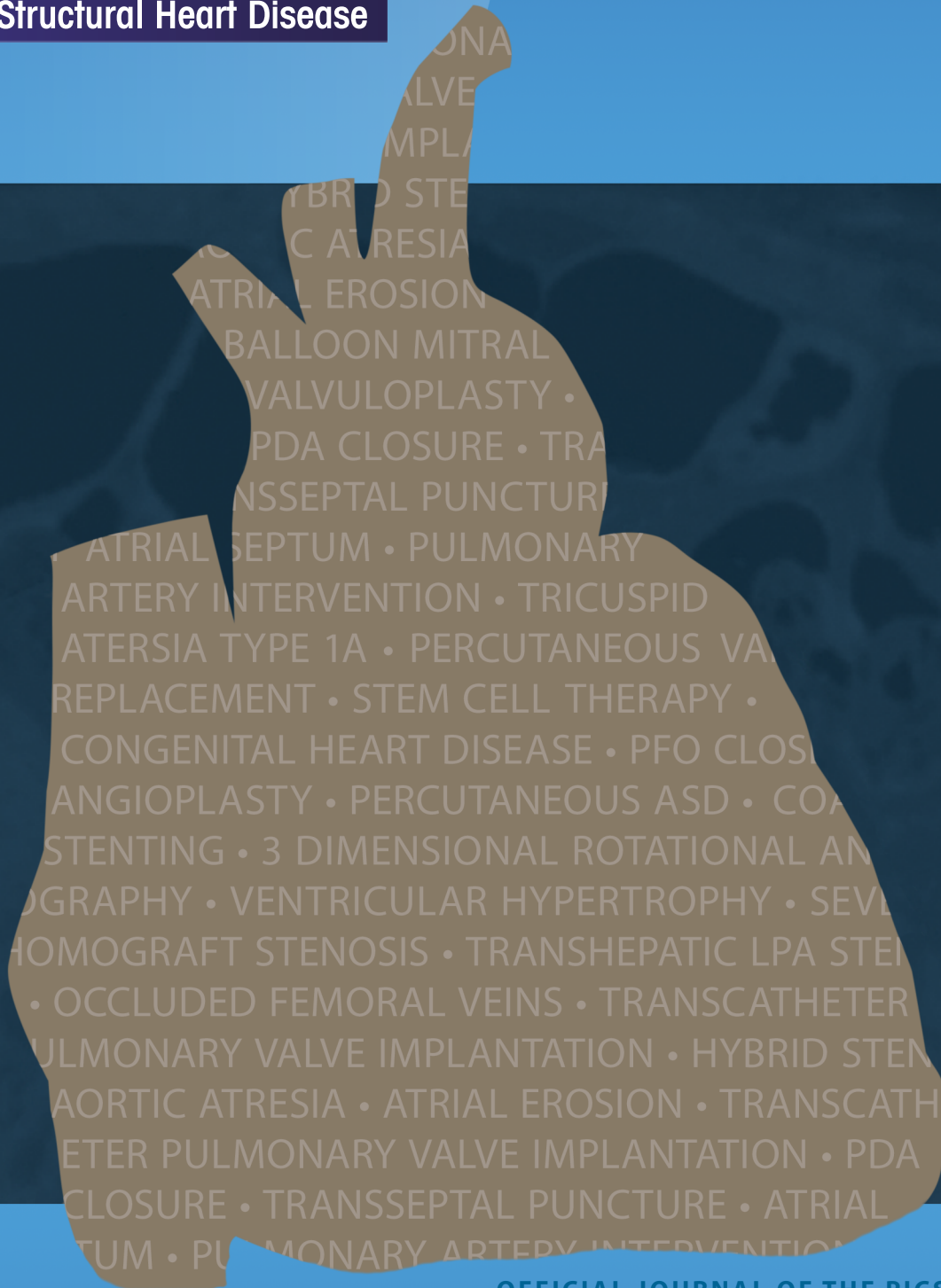


JSHD

Journal of Structural Heart Disease

Publish Date:

October 2019
Volume 5, Issue 5



OFFICIAL JOURNAL OF THE PICS FOUNDATION
PICS Foundation
PEDIATRIC AND ADULT INTERVENTIONAL CARDIAC SYMPOSIUM



Published by
SCIENCE INTERNATIONAL CORP.
ISSN 2325-4637

Now accepting papers at <https://structuralheartdisease.com>.



Committed to Advancing Transcatheter Heart Valve Therapy

Edwards SAPIEN XT Transcatheter Heart Valve

Approved for Pulmonic Procedures

The SAPIEN XT valve is approved for pulmonic procedures in pediatric and adult patients with a dysfunctional, non-compliant right ventricular outflow tract (RVOT) conduit.

SAPIEN XT Valve Sizing—Pulmonic

23 mm	26 mm	29 mm
20-23 mm	23-26 mm	26-29 mm

Diameter of intended location within the conduit

Edwards Lifesciences is driving the innovation, collaboration, and education needed to bring transcatheter technology to more patients worldwide.

» Visit [Edwards.com/pulmonic](https://www.edwards.com/pulmonic) for more information

See adjacent page for Important Safety Information.

CAUTION: Federal (United States) law restricts this device to sale by or on the order of a physician.

Edwards, Edwards Lifesciences, the stylized E logo, Edwards SAPIEN, Edwards SAPIEN XT, SAPIEN, and SAPIEN XT are trademarks of Edwards Lifesciences Corporation. All other trademarks are the property of their respective owners.

© 2017 Edwards Lifesciences Corporation. All rights reserved. PP--US-1832 v1.0

Edwards Lifesciences • One Edwards Way, Irvine CA 92614 USA • [edwards.com](https://www.edwards.com)



Edwards

Important Safety Information

EDWARDS SAPIEN XT TRANSCATHETER HEART VALVE WITH THE NOVAFLEX+ DELIVERY SYSTEM – PULMONIC

Indications: The Edwards SAPIEN XT transcatheter heart valve (THV) systems are indicated for use in pediatric and adult patients with a dysfunctional, non-compliant right ventricular outflow tract (RVOT) conduit with a clinical indication for intervention and: pulmonary regurgitation \geq moderate and/or mean RVOT gradient \geq 35 mmHg.

Contraindications: The THV and delivery systems are contraindicated in patients with inability to tolerate an anticoagulation/antiplatelet regimen or who have active bacterial endocarditis.

Warnings: The devices are designed, intended, and distributed for single use only. **Do not resterilize or reuse the devices.** There are no data to support the sterility, nonpyrogenicity, and functionality of the devices after reprocessing. Assessment for coronary compression risk prior to valve implantation is essential to prevent the risk of severe patient harm. Incorrect sizing of the THV may lead to paravalvular leak, migration, embolization and/or RVOT rupture. Accelerated deterioration of the THV may occur in patients with an altered calcium metabolism. Prior to delivery, the THV must remain hydrated at all times and cannot be exposed to solutions other than its shipping storage solution and sterile physiologic rinsing solution. THV leaflets mishandled or damaged during any part of the procedure will require replacement of the THV. Do not use the THV if the tamper evident seal is broken, the storage solution does not completely cover the THV, the temperature indicator has been activated, the THV is damaged, or the expiration date has elapsed. Do not mishandle the NovaFlex+ delivery system or use it if the packaging or any components are not sterile, have been opened or are damaged (e.g. kinked or stretched), or the expiration date has elapsed. Use of excessive contrast media may lead to renal failure. Measure the patient's creatinine level prior to the procedure. Contrast media usage should be monitored. Patient injury could occur if the delivery system is not un-flexed prior to removal. Care should be exercised in patients with hypersensitivities to cobalt, nickel, chromium, molybdenum, titanium, manganese, silicon, and/or polymeric materials. The procedure should be conducted under fluoroscopic guidance. Some fluoroscopically guided procedures are associated with a risk of radiation injury to the skin. These injuries may be painful, disfiguring, and long-lasting. THV recipients should be maintained on anticoagulant/antiplatelet therapy as determined by their physician. This device has not been tested for use without anticoagulation. Do not add or apply antibiotics to the storage solution, rinse solutions, or to the THV.

Precautions: Safety, effectiveness, and durability of the THV have not been established for implantation within a previously placed surgical or transcatheter pulmonic valve. Long-term durability has not been established for the THV. Regular medical follow-up is advised to evaluate THV performance. Glutaraldehyde may cause irritation of the skin, eyes, nose and throat. Avoid prolonged or repeated exposure to, or breathing of, the solution. Use only with adequate ventilation. If skin contact occurs, immediately flush the affected area with water; in the event of contact with eyes, immediately flush the affected area with water and seek immediate medical attention. For more information about glutaraldehyde exposure, refer to the Material Safety Data Sheet available from Edwards Lifesciences. Patient anatomy should be evaluated to prevent the risk of access that would preclude the delivery and deployment of the device. To maintain proper valve leaflet coaptation, do not overinflate the deployment balloon. Appropriate antibiotic prophylaxis is recommended post-procedure in patients at risk for prosthetic valve infection and endocarditis. Safety and effectiveness have not been established for patients with the following characteristics/comorbidities: Echocardiographic evidence of intracardiac mass, thrombus, or vegetation; a known hypersensitivity or contraindication to aspirin, heparin or sensitivity to contrast media, which cannot be adequately premedicated; pregnancy; and patients under the age of 10 years.

Potential Adverse Events: Potential risks associated with the overall procedure including potential access complications associated with standard cardiac catheterization, balloon valvuloplasty, the potential risks of conscious sedation and/or general anesthesia, and the use of angiography: death; respiratory insufficiency or respiratory failure; hemorrhage requiring transfusion or intervention; cardiovascular injury including perforation or dissection of vessels, ventricle, myocardium or valvular structures that may require intervention; pericardial effusion or cardiac tamponade; embolization including air, calcific valve material or thrombus; infection including septicemia and endocarditis; heart failure; myocardial infarction; renal insufficiency or renal failure; conduction system defect arrhythmia; arteriovenous fistula; reoperation or reintervention; ischemia or nerve injury; pulmonary edema; pleural effusion, bleeding; anemia; abnormal lab values (including electrolyte imbalance); hypertension or hypotension; allergic reaction to anesthesia, contrast media, or device materials; hematoma or ecchymosis; syncope; pain or changes at the access site; exercise intolerance or weakness; inflammation; angina; fever. Additional potential risks associated with the use of the THV, delivery system, and/or accessories include: cardiac arrest; cardiogenic shock; emergency cardiac surgery; coronary flow obstruction/transvalvular flow disturbance; device thrombosis requiring intervention; valve thrombosis; device embolization; device malposition requiring intervention; valve deployment in unintended location; structural valve deterioration (wear, fracture, calcification, leaflet tear/tearing from the stent posts, leaflet retraction, suture line disruption of components of a prosthetic valve, thickening, stenosis); paravalvular or transvalvular leak; valve regurgitation; hemolysis; device explants; nonstructural dysfunction; and mechanical failure of delivery system, and/or accessories.

Edwards Crimper

Indications: The Edwards crimper is indicated for use in preparing the Edwards SAPIEN XT transcatheter heart valve for implantation.

Contraindications: No known contraindications.

Warnings: The device is designed, intended, and distributed for single use only. **Do not resterilize or reuse the device.** There are no data to support the sterility, nonpyrogenicity, and functionality of the device after reprocessing. Do not mishandle the device. Do not use the device if the packaging or any components are not sterile, have been opened or are damaged, or the expiration date has elapsed.

Precautions: For special considerations associated with the use of this device prior to THV implantation, refer to the SAPIEN XT transcatheter heart valve Instructions for Use.

Potential Adverse Events: No known potential adverse events.

CAUTION: Federal (United States) law restricts this device to sale by or on the order of a physician.

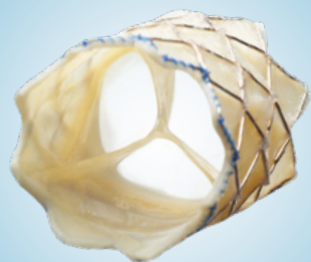
Edwards, Edwards Lifesciences, the stylized E logo, Edwards SAPIEN, Edwards SAPIEN XT, NovaFlex, NovaFlex+, SAPIEN, and SAPIEN XT are trademarks or service marks of the Edwards Lifesciences Corporation. All other trademarks are the property of their respective owners.

© 2017 Edwards Lifesciences Corporation. All rights reserved. PP-US-1832 v1.0

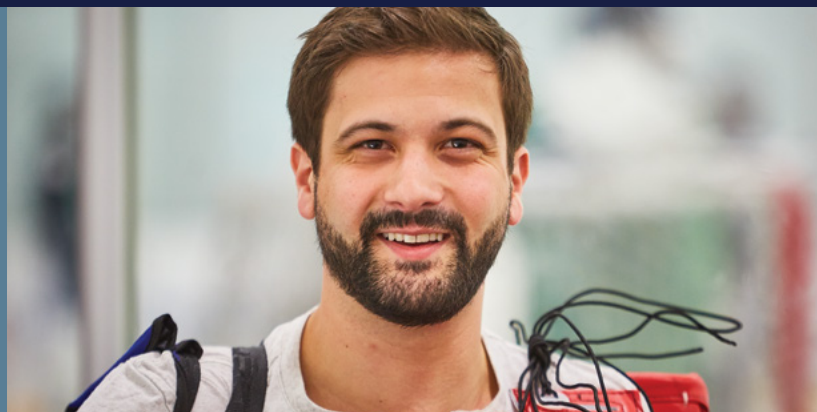
Edwards Lifesciences • One Edwards Way, Irvine CA 92614 USA • edwards.com



RIGHT DATA.



Melody™
Transcatheter Pulmonary
Valve (TPV) System



Proven to Delay
Conduit Replacement

88.8%

freedom from reoperation*
*USIDE Study

Proven Valve
Competence

98.1%

of subjects with \leq mild PR*

Designed Specifically for Pulmonary Valve Replacement

The Melody valve is the longest studied transcatheter pulmonary valve at seven years post-implant.

The Melody TPV System first received CE mark in September 2006.

The Melody TPV System received Health Canada approval in December 2006 and US approval under an HDE on January 25, 2010 (H080002).

PMA approval received January 27, 2015 (P140017).

©2018 Medtronic. All rights reserved.
UC201900307 EN 05/2018

Medtronic
Further, Together

Melody™ Transcatheter Pulmonary Valve, Ensemble™ II Transcatheter Valve Delivery System

Important Labeling Information for the United States

Indications: The Melody TPV is indicated for use in the management of pediatric and adult patients who have a clinical indication for intervention on a dysfunctional right ventricular outflow tract (RVOT) conduit or surgical bioprosthetic pulmonary valve that has \geq moderate regurgitation, and/or a mean RVOT gradient \geq 35 mm Hg.

Contraindications: None known.

Warnings/Precautions/Side Effects:

- **DO NOT implant in the aortic or mitral position. Pre-clinical bench testing of the Melody valve suggests that valve function and durability will be extremely limited when used in these locations.**
- DO NOT use if patient's anatomy precludes introduction of the valve, if the venous anatomy cannot accommodate a 22 Fr size introducer, or if there is significant obstruction of the central veins.
- DO NOT use if there are clinical or biological signs of infection including active endocarditis. Standard medical and surgical care should be strongly considered in these circumstances.
- Assessment of the coronary artery anatomy for the risk of coronary artery compression should be performed in all patients prior to deployment of the TPV.
- To minimize the risk of conduit rupture, do not use a balloon with a diameter greater than 110% of the nominal diameter (original implant size) of the conduit for pre-dilation of the intended site of deployment, or for deployment of the TPV.
- The potential for stent fracture should be considered in all patients who undergo TPV placement. Radiographic assessment of the stent with chest radiography or fluoroscopy should be included in the routine postoperative evaluation of patients who receive a TPV.
- If a stent fracture is detected, continued monitoring of the stent should be performed in conjunction with clinically appropriate hemodynamic assessment. In patients with stent fracture and significant associated RVOT obstruction or regurgitation, reintervention should be considered in accordance with usual clinical practice.

Potential procedural complications that may result from implantation of the Melody device include the following: rupture of the RVOT conduit, compression of a coronary artery, perforation of a major blood vessel, embolization or migration of the device, perforation of a heart chamber, arrhythmias, allergic reaction to contrast media, cerebrovascular events (TIA, CVA), infection/sepsis, fever, hematoma, radiation-induced erythema, blistering, or peeling of skin, pain, swelling, or bruising at the catheterization site.

Potential device-related adverse events that may occur following device implantation include the following: stent fracture, stent fracture resulting in recurrent obstruction, endocarditis, embolization or migration of the device, valvular dysfunction (stenosis or regurgitation), paravalvular leak, valvular thrombosis, pulmonary thromboembolism, hemolysis.

*The term "stent fracture" refers to the fracturing of the Melody TPV. However, in subjects with multiple stents in the RVOT it is difficult to definitively attribute stent fractures to the Melody frame versus another stent.

For additional information, please refer to the Instructions for Use provided with the product or available on <http://manuals.medtronic.com>.

CAUTION: Federal law (USA) restricts this device to sale by or on the order of a physician.

Important Labeling Information for Geographies Outside of the United States

Indications: The Melody™ TPV is indicated for use in patients with the following clinical conditions:

- Patients with regurgitant prosthetic right ventricular outflow tract (RVOT) conduits or bioprostheses with a clinical indication for invasive or surgical intervention, OR
- Patients with stenotic prosthetic RVOT conduits or bioprostheses where the risk of worsening regurgitation is a relative contraindication to balloon dilatation or stenting

Contraindications:

- Venous anatomy unable to accommodate a 22 Fr size introducer sheath
- Implantation of the TPV in the left heart
- RVOT unfavorable for good stent anchorage
- Severe RVOT obstruction, which cannot be dilated by balloon
- Obstruction of the central veins
- Clinical or biological signs of infection
- Active endocarditis
- Known allergy to aspirin or heparin
- Pregnancy

Potential Complications/Adverse Events: Potential procedural complications that may result from implantation of the Melody device include the following: rupture of the RVOT conduit, compression of a coronary artery, perforation of a major blood vessel, embolization or migration of the device, perforation of a heart chamber, arrhythmias, allergic reaction to contrast media, cerebrovascular events (TIA, CVA), infection/sepsis, fever, hematoma, radiation-induced erythema, pain, swelling or bruising at the catheterization site.

Potential device-related adverse events that may occur following device implantation include the following: stent fracture, stent fracture resulting in recurrent obstruction, endocarditis, embolization or migration of the device, valvular dysfunction (stenosis or regurgitation), paravalvular leak, valvular thrombosis, pulmonary thromboembolism, hemolysis.

The term "stent fracture" refers to the fracturing of the Melody TPV. However, in subjects with multiple stents in the RVOT it is difficult to definitively attribute stent fractures to the Melody frame versus another stent.

For additional information, please refer to the Instructions for Use provided with the product or available on <http://manuals.medtronic.com>.

The Melody Transcatheter Pulmonary Valve and Ensemble II Transcatheter Delivery System has received CE Mark approval and is available for distribution in Europe.

medtronic.com

710 Medtronic Parkway
Minneapolis, MN 55432-5604
USA
Tel: (763) 514-4000
Fax: (763) 514-4879
Toll-free: (800) 328-2518

LifeLine
CardioVascular Technical Support
Tel: (877) 526-7890
Tel: (763) 526-7890
Fax: (763) 526-7888
rs.cstechsupport@medtronic.com

Made possible.

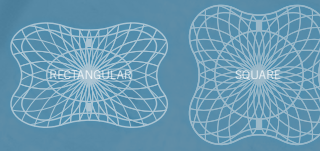
Made For life



Working together to understand your needs and challenges drives valuable outcomes that positively impact you and your patients' future.

Canon Medical's vision and commitment to improving life for all, lies at the heart of everything we do. By partnering to focus on what matters, together we can deliver intelligent, high quality solutions.

With Canon Medical, true innovation is **made possible**.



Occlutech Paravalvular Leak Device

Paravalvular leak closure

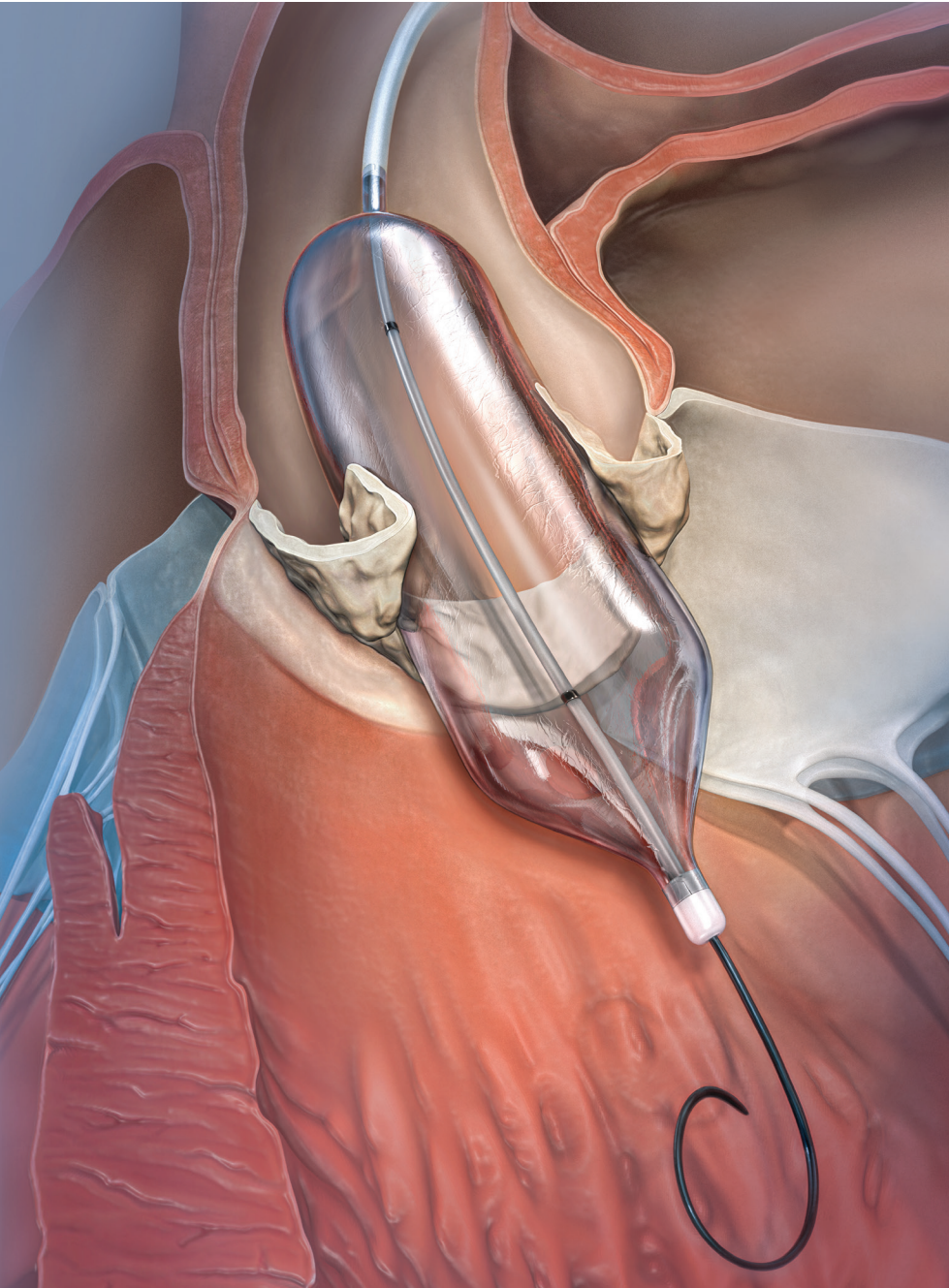
The Occlutech PLD is an ideal device for closing paravalvular leaks as it offers a range of outstanding features

- User-friendly and easy to use.
- Optimal positioning by two gold markers.
- Repositionable and fully retrievable.
- Optimized concave shape facilitates placement around the implanted valve.
- Available with wide range of sizes for closing from small leaks to large leaks.
- Available with different design options for different PVL morphologies: Rectangular and Square.



The Occlutech PLD is available with two types of connections between the discs, **Waist** or **Twist**. Example shown on a Occlutech PLD Square.








ESTABLISHED.

PROVEN.

EFFECTIVE.

For over 25 years, B. Braun Interventional Systems has been and continues to be a trusted industry leader in providing high quality valvuloplasty brands. Z-MED and Z-MED II are proven brands with excellent product features for dependable performance and procedural efficiency.

-  Rapid inflation/deflation times maximize reperfusion and minimize procedure time
-  Short balloon tapers and distal tip for optimal positioning within the valve
-  Low profile design provides consistent deliverability and retractability

Z-MED™ and Z-MED II™

Balloon Aortic and Pulmonic Valvuloplasty Catheters

Distributed by:
B. Braun Interventional Systems Inc. | Part of the B. Braun Group of Companies
Bethlehem, PA | USA | 877-836-2228 | www.bisusa.org

Editorial Board

Editor-in-Chief

Ziyad M. Hijazi Sidra Medical & Research Center
(Doha-qatar)

Co-Editor-in-Chief

Oscar Mendiz Fundacion Favaloro
(Buenos Aires, Argentina)

Assistant Editors

Damien Kenny Rush University Medical Center
(Chicago, IL)

Editorial Board

Teiji Akagi Okayama University
(Okayama, Japan)

Bagratt Alekyan Bakoulev Scientific Center for
Cardiovascular Surgery
(Moscow, Russia)

Zahid Amin Children's Hospital of Georgia
(Augusta, GA)

Steven Bailey University of Texas, San Antonio
(San Antonio, TX)

Lee Benson Hospital for Sick Kids
(Toronto, Canada)

Lisa Bergersen Boston Children's Hospital
(Boston, MA)

Younes Boudjemline Hospital Necker
(Paris, France)

Elchanan Bruckheimer Schneider's Children's
Medical Center
(Petach Tikva, Israel)

Maurice Buckbinder Stanford University
(Palo Alto, CA)

Massimo Caputo Rush University Medical Center
(Chicago, IL)

Mario Carminati San Donato Milanese
(Milan, Italy)

John Carroll University of Colorado Denver
(Aurora, CO)

John P. Cheatham Ohio State University
(Columbus, OH)

Jae Young Choi Severance Cardiovascular Hospital
(Seoul, Korea)

Antonio Colombo St. Raffaele Hospital
(Milan, Italy)

Costantino Costantini Hospital Cardiológico Costantini
(Curitiba, Brazil)

Alain Cribier Charles Nicolle Hospital
(Rouen, France)

Roberto Cubeddu Aventura Hospital
(Miami, FL)

Bharat Dalvi Glenmark Cardiac Centre
(Mumbai, India)

Associate Editors

Clifford J. Kavinsky Rush University Medical Center
(Chicago, IL)

Bray Patrick Lake PFO Research Foundation
(Boulder, CO)

John Messenger University of Colorado
(Aurora, CO)

Managing Editor

Hussam Suradi Rush University Medical Center
(Chicago, IL)

Jo De Giovanni Birmingham Children's Hospital
(Birmingham, United Kingdom)

Helene Eltchanninof University Hospital
(Rouen, France)

Maiy El Syed Ain Shams Univesity
(Cairo, Egypt)

Thomas Fagan University of Colorado
(Denver, CO)

Ted Feldman Evanston Northshore Hospital
(Evanston, IL)

Olaf Franzen University Heart Center Hamburg
(Hamburg, Germany)

Yun Ching Fu Taichung Veterans General Hospital
(Taichung, Taiwan)

David Gao Shanghai Children's Medical Center
(Shanghai, China)

Eulogio Garcia Hospital Clinico San Carlos
(Madrid, Spain)

Marc Gewillig University of Lueven
(Lueven, Belgium)

Matt Gillespie Children's Hospital of Philadelphia
(Philadelphia, PA)

Omer Goktekin BezmiAlem Vakif University
(Istanbul, Turkey)

Steven Goldberg University of Washington
(Seattle, WA)

William Gray Columbia University
(New York, NY)

Eberhard Grube Heart Center Siegburg
(Siegburg, Germany)

Jeff Harrisberg Pediatric Cardiology
(Gauteng, South Africa)

William E. Hellenbrand Yale University
(New Haven, CT)

James Hermiller The Care Group
(Indianapolis, IN)

Howard Herrmann University of Pennsylvania
(Philadelphia, PA)

David Holmes Mayo Clinic
(Rochester, MN)

Noa Holoshitz	Rush University Medical Center (Chicago, IL)	Raj Makkar	Cedars Sinai Medical Center (Los Angeles, CA)
Ralf Holzer	Sidra Medical & Research Center (Doha, Qatar)	Robert March	Rush University Medical Center (Chicago, IL)
Eric Horlick	University of Toronto (Toronto, Canada)	Gwen Mayes	VP National Patient Advocate Foundation (Washington, DC)
Reda Ibrahim	Montreal Heart Institute (Montreal, Canada)	Pat McCarthy	Northwestern Memorial Hospital (Chicago, IL)
Michel Ilbawi	Rush University Medical Center (Chicago, IL)	Doff McElhinney	New York University (New York, NY)
Frank Ing	LA Children's Hospital (Los Angeles, CA)	John Messenger	University of Colorado (Denver, CO)
Alexander Javois	Hope Children's Hospital (Oak Lawn, IL)	Friedrich Mohr	Herzzentrum Universitaet Leipzig (Leipzig, Germany)
Thomas Jones	Seattle Children's Hospital (Seattle, WA)	Issam Moussa	(Jacksonville, FL)
Saibal Kar	Cedars Sinai Medical Center (Los Angeles, CA)	Michael Mullen	The Heart Hospital (London, England)
Clifford Kavinsky	Rush University Medical Center (Chicago, IL)	David Muller	St. Vincent's Hospital (Sydney, Australia)
Joseph Kay	University of Colorado (Denver, CO)	William O'Neill	Henry Ford Hospital (Detroit, MI)
Damien Kenny	Rush University Medical Center (Chicago, IL)	Igor Palacios	Mass General Hospital (Boston, MA)
Morton Kern	University of California Irvine (Irvine, CA)	SJ Park	University of Ulsan College of Medicine (Seoul, Korea)
Michael Kim	University of Colorado (Aurora, CO)	Carlos Pedra	Danta Pazzanese Instituto de Cardiologia (Sao Paulo, Brazil)
Seong-Ho Kim	Cheju Halla General Hospital (South Korea)	Alejandro Peirone	Children's Hospital of Cordoba (Cordoba, Argentina)
Susheel Kodali	Columbia University Medical Center (New York, NY)	Giacomo Pongiglione	Bambino Gesu Hospital (Rome, Italy)
Jackie Kreutzer	Pittsburgh Children's Hospital (Pittsburgh, PA)	Matthew Price	Scripps Clinic (La Jolla, CA)
Shelby Kutty	Children's Hospital and University of Nebraska Medical Center (Omaha, NB)	Robert Quaife	University of Colorado (Denver, CO)
Bray Patrick-Lake	PFO Research Foundation (Boulder, CO)	Shakeel Qureshi	Evelina Children's Hospital (London, UK)
Michael Landzberg	Boston Children's Hospital (Boston, MA)	Steve Ramee	Oschner Clinic (New Orleans, LA)
Roberto Lang	University of Chicago Medical Center (Chicago, IL)	Mark Reisman	Swedish Medical Center (Seattle, WA)
John Lasala	Barnes Jewish Hospital, Washington University (St. Louis, MO)	John Rhodes	Miami Children's Hopsital (Miami, FL)
Martin B. Leon	Columbia University (New York, NY)	Charanjit Rihal	Mayo Clinic (Rochester, MN)
Daniel Levi	UCLA Medical Center (Los Angeles, CA)	Richard Ringel	Johns Hopkins Medical Center (Baltimore, MD)
Scott Lim	University of Virginia Health System (Charlottesville, VA)	Carlos Ruiz	Lenox Hill Hospital (New York, NY)
Michael Mack	Baylor Healthcare System (Plano, TX)	Ernesto Salcedo	University of Colorado (Denver, CO)
Francesco Maisano	University of Zurich (Zurich, Switzerland)	Joachim Schofer	Hamburg University Cardiovascular Center (Hamburg, Germany)

Horst Sievert	CardioVascular Center Sankt Katharinen Hospital (Frankfurt, Germany)		Medical School (Camden, NJ)
Frank Silvestry	University of Pennsylvania Hospital (Philadelphia, PA)	Alec Vahanian	Bichat University Hospital (Paris, France)
Paul Sorajja	Minneapolis Heart Institute Foundation (Minneapolis, MN)	Joseph J. Vettukattil	Spectrum Health (Grand Rapids, MI)
Christian Spies	Queen's Heart Physician Practice (Honolulu, HI)	Kevin Walsh	Our Lady's Hospital (Dublin, Ireland)
Gregg Stone	Columbia University (New York, NY)	John Webb	St. Paul Hospital Vancouver (British Columbia, Canada)
Corrado Tamborino	University of Catania (Catania, Italy)	Brian Whisenant	Intermountain Medical Center (Salt Lake City, Utah)
Vinod Thourani	Emory University (Atlanta, GA)	Matthew Williams	Mount Sinai Medical Center (New York, NY)
Jonathan Tobis	UCLA Medical Center (Los Angeles, CA)	Neil Wilson	University of Colorado (Denver, CO)
Murat Tuczu	Cleveland Clinic Foundation (Cleveland, OH)	Evan Zahn	Cedars Sinai Medical Center (Los Angeles, CA)
Zoltan Turi	Robert Wood Johnson		

ORIGINAL SCIENTIFIC ARTICLES

206 Difference Among Embolic Sources Between Younger and Older Patients With Stroke of Undetermined Source on Routine Diagnostic Assessment Including Transesophageal Echocardiography

Hiroya Takafuji, Shinobu Hosokawa, Riyo Ogura, Yoshikazu Hiasa

213 Assessment of the Dynamism of the Left Atrial Appendage Dimensions: A Computer Tomographic Analysis

Mohamed Marwan, Amina Vaillant, Fabian Ammon, Daniel Bittner, Michaela Hell, Stephan Achenbach

NEW TECHNOLOGY

221 Transcatheter Trans-aortic Retrograde Approach for the Closure of Perimembranous Ventricular Septal Defects using Cocoon [Amplatzer Duct Occluder I Like] Device – An Initial Experience from a Single Centre

Pankaj Jariwala, Kumar Narayanan, Edla Arjun Padma Kumar

CASE REPORT

229 Entrapped Stent Delivery Catheter Shaft After High Risk TAVI: Retrieval & Lessons Learned

Safwan Kassas, Peter Fattal, Manoj Sharma

Journal of Structural Heart Disease (ISSN 2325-4637) is an online open-access journal issued bi-monthly (6 issues per year, one volume per year) by Science International Corporation.

All correspondence should be directed to: Ziyad M. Hijazi, MD, Editor-in-Chief, Journal of Structural Heart Disease, PO Box 26999, Doha, Qatar. Tel.: +974-4003-6601, E-Mail: jshd@scienceinternational.org

All inquiries regarding copyrighted material from this publication should be directed to Science International Corporation: 70 Forest Street, Suite 6-C, Stamford, CT, 06901, USA. Tel.: +1-203-329-8842, Fax: +1-203-329-8846, E-Mail: skorn@scienceinternational.org

Difference Among Embolic Sources Between Younger and Older Patients with Stroke of Undetermined Source on Routine Diagnostic Assessment Including Transesophageal Echocardiography

Hiroya Takafuji, MD*, Shinobu Hosokawa, MD, Riyo Ogura, MD, Yoshikazu Hiasa, MD

Department of Cardiology, Tokushima Red Cross Hospital, Komatsushima, Tokushima, Japan

Abstract

Background: The distribution of embolic sources in patients with embolic stroke of undetermined source (ESUS) remains unclear. Furthermore, the difference among embolic sources according to age is unknown. The aim of this study was to identify the distribution of embolic sources in younger and older patients with embolic strokes who underwent routine diagnostic assessment with transesophageal echocardiography (TEE) and to evaluate the distribution of paradoxical embolism related to patent foramen ovale (PFO) between younger and older.

Methods and Results: Between May 2012 and December 2017, 102 ESUS patients underwent routine diagnostic assessment including TEE at our hospital to identify the specific cause of their embolic stroke. We compared the causes of embolic stroke between younger (<60 years; mean age, 49.3 ± 10.9 years; $n=24$) and older (>60 years; mean age, 74.8 ± 6.2 years; $n=78$) patients. Older patients had significantly higher rates of aortic arch atherosclerotic plaques (4.2% vs. 48.7%; $p < 0.001$). The other causes were not significantly different between the two groups. Especially in paradoxical embolism related to PFO, younger patients had fewer other embolic sources in addition to PFO or both PFO and atrial septal aneurysm (ASA) than older patients. However,

older patients also exhibited PFO or both PFO and ASA (32.6%) without other embolic sources.

Conclusions: Our study suggests that embolic source of ESUS to undergo routine diagnostic assessment including transesophageal echocardiography (TEE) is similar between younger and older. However, the total numbers of embolic sources is significantly higher in older patients. In paradoxical embolism related to PFO, 33% of older patients had no other identifiable cause of embolic stroke besides a PFO.

Copyright © 2019 Science International Corp.

Key Words

Embolic stroke of undetermined source • Age • Patent foramen ovale

Introduction

Embolic stroke of undetermined source (ESUS) is a form of stroke defined based on a set of criteria proposed by the Cryptogenic Strokes/ESUS International Working Group [1]. Although the causes of ESUS have been previously reported in multiple studies, the cause of stroke could not be identified using the ESUS criteria in a number of patients. Moreover, this

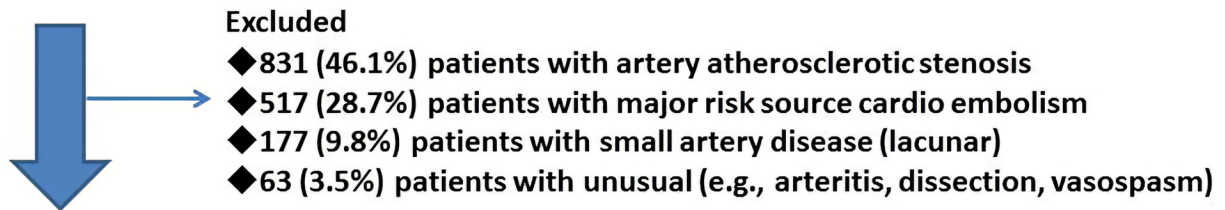


Method

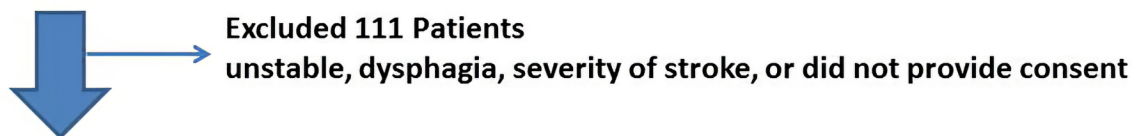
Study design: single-center, retrospective study

Term: May 2012 – December 2017

1801 patients with acute ischemic stroke



213 patients (11.8%) with ESUS



102 patients (24 Younger patients: ≤ 60 years, 78 Older patients: > 60 years) with ESUS who underwent routine diagnostic assessment including TEE

Figure 1. Study flowchart. ESUS: embolic stroke of undetermined sources; TEE: transesophageal echocardiography.

proposed diagnostic assessment for ESUS does not include routine use of transesophageal echocardiography (TEE).

Patent foramen ovale (PFO) is one of the causes of ESUS, especially in patients with paradoxical embolism. The relationship between paradoxical embolism and PFO is well documented. Conversely, the gold standard imaging tool in diagnosing PFO is TEE. In addition, percutaneous closure of PFO in patients with embolic strokes was recently deemed to be more effective than medical therapy alone [2, 3, 18]. In the current era of PFO closure, it is important to determine the specific embolic source. However, the distribution of embolic sources in patients with ESUS remains unclear. Additionally, the difference in embolic sources in patients with different ages is

not well described. The aim of the present study was to investigate the distribution of embolic sources in patients with embolic strokes according to their age using routine diagnostic assessments including TEE and to evaluate the distribution of paradoxical embolism related to patent foramen ovale (PFO) between younger and older..

Materials and Methods

This was a single-center, retrospective study. Between May 2012 and December 2017, 1801 consecutive patients with acute ischemic stroke were admitted to the Tokushima Red Cross Hospital in Japan. Figure 1 shows the study flowchart. Of these 1801 patients, 213 (11.8%) fulfilled the ESUS diag-

Table 1. Patient characteristics according to age

	All patients (n=102)	Younger (n=24)	Older (n=78)	P value
Age, yrs	68.8±13.2	49.3±10.9	74.8±6.2	<0.001
Body mass index, kg/m ²	23.1±3.1	23.8±3.4	22.9±3.0	0.21
Male	71(69.6)	17(70.8)	54(69.2)	0.88
Hypertension	64(62.7)	7(29.2)	57(73.1)	<0.001
Diabetes mellitus	27(26.5)	7(29.2)	20(25.6)	0.73
Dyslipidemia	62(60.1)	15(62.5)	47(60.3)	0.84
Smoking history	53(51.9)	15(62.5)	38(48.7)	0.24
Previous stroke	18(17.6)	3(12.5)	15(19.2)	0.45
Af history	0(0)	0(0)	0(0)	-

Values are mean±SD, n (%).

Af: atrial fibrillation

nostic criteria and were classified according to the cause of embolic stroke [1]. Based on joint decision by a neurologist and cardiologist, 102 patients underwent routine diagnostic assessment with additional TEE to determine the specific cause of their embolic stroke. Patients who were unstable or did not provide consent were excluded. Moreover, we compared the cause of embolic stroke between younger (≤ 60 years; mean age, 49.3 ± 10.9 years; age range, 23–60 years; $n=24$) and older (>60 years; mean age, 74.8 ± 6.2 years; age range, 62–86 years; $n=78$) patients.

TEE examination and definitions of cardiac sources of embolism

TEE was performed to determine the specific embolic source, in addition to routine diagnostic assessment. An IE33 echocardiography system (Philips Medical Systems, Eindhoven, The Netherlands) with a multiplane transesophageal 5-MHz transducer was used. TEE was performed under sedation, and embolic sources were diagnosed by consensus of two experienced echocardiography specialists. PFO was defined as the presence of a right-to-left shunt using agitated saline contrast microbubbles within three cardiac cycles via a Valsalva maneuver with abdominal compression after complete opacification of the right atrium. TEE for detection of PFO was performed at the end of the examination after the anesthetic

wore off. Atrial septal aneurysms (ASAs) were defined as an interatrial septum with a 10 mm protrusion into the right or left atrium and a diameter ≥ 15 mm at the base of the aneurysm. Reduced left atrial appendage blood flow (LAAF) was defined as <30 cm/sec. Aortic plaque was defined as plaque thickness >4 mm in the aortic arch or descending aorta. The total number of embolic sources was used to calculate the risk of stroke according to the ESUS criteria for embolic stroke [1].

Statistical analysis

Continuous variables are expressed as mean \pm standard deviation. Categorical variables were compared between groups using the chi-squared or Fisher's exact tests. A $p < 0.05$ was considered statistically significant. All data were analyzed using JMP version 8 (SAS Institute, Cary, NC).

Ethical approval

This present study has been approved by ethics standards of the institutional research, and the study was performed in accordance with the 1964 Declaration of Helsinki.

Results

Baseline characteristics

The baseline characteristics of the younger and older patients are shown in Table 1. The mean age of patients in this study was 68.8 ± 13.2 years and 71 (69.9%) were male. Compared with the younger patients, the rates of hypertension were significantly higher in the older patients. The prevalence of diabetes mellitus, dyslipidemia, smoking history, and previous stroke were similar between the younger and older patients. None of the patients in either group had a history of atrial fibrillation or flutter.

Distribution of embolic sources in patients with ESUS according to age

The various embolic sources are summarized in Table 2. The most frequent cause of embolic stroke was PFO (56.9%), followed by aortic arch atherosclerotic plaques (38.2%). No significant differences between the groups were found in the rates of minor-risk potential cardio embolic sources such as the

Table 2: Characteristics of the embolic sources.

Causes	All patients (n=102)	Younger (n=24)	Older (n=78)	P value
Minor-risk potential cardio embolic sources				
<i>Mitral valve</i>				
Myxomatous valvulopathy with prolapse (%)	1(0.9)	0(0)	1(1.3)	0.57
Mitral annular calcification (%)	3(2.9)	1(4.2)	2(2.6)	0.68
<i>Aortic valve</i>				
Aortic valve stenosis (%)	1(0.9)	0(0)	1(1.3)	0.57
Calcific aortic valve (%)	14(13.7)	1(4.2)	13(16.7)	0.12
<i>Non-atrial fibrillation atrial dysrhythmias and stasis</i>				
Atrial asystole and sick sinus syndrome (%)	2(1.9)	0(0)	2(2.6)	0.43
Atrial appendage stasis with reduced flow velocities or spontaneous echo densities (%)	5(4.9)	0(0)	5(6.4)	0.20
<i>Atrial structural abnormalities</i>				
Atrial septal aneurysm (%)	32(31.4)	4(16.7)	28(35.9)	0.07
Chiari network (%)	11(10.8)	1(4.2)	10(12.8)	0.23
<i>Left ventricle</i>				
Moderate systolic or diastolic dysfunction, Ventricular non-compaction, Endomyocardial fibrosis (%)	9(8.8)	2(8.3)	7(9.0)	0.92
Cancer-associated				
Convert non-bacterial thrombotic endocarditis , Tumor emboli from occult cancer (%)	4(3.9)	0(0)	4(5.1)	0.26
Arteriogenic emboli				
Aortic arch atherosclerotic plaques, Cerebral artery non-stenotic plaques with ulceration (%)	39(38.2)	1(4.2)	38(48.7)	<0.001
Paradoxical embolism				
Patent foramen ovale (%)	58(56.9)	15(62.5)	43(55.1)	0.52
Atrial septal defect (%)	3(2.9)	1(4.2)	2(2.6)	0.68
Pulmonary arteriovenous fistula (%)	0(0)	0(0)	0(0)	-

mitral valve, aortic valve, atrial structural abnormalities, and left ventricle. Similarly, no difference in cancer-associated and paradoxical emboli was observed between younger and older patients. PFO as the embolic source was also similar between younger and older patients (62.5% vs. 55.1%, $p=0.52$). On the other hand, the rate of aortic arch atherosclerotic plaques was significantly higher in older patients (4.2% vs. 48.7%, $p < 0.001$).

Total numbers of other embolic sources in addition to PFO or combined PFO and ASA

A total of 58 patients (56.9%) were detected PFO. Table 3 presents the total number of other embolic sources in addition to PFO or combined PFO and ASA. Older patients exhibited multiple causes of embolic stroke more frequently than younger patients with only 14 of 43 (32.6%) having PFO or combined PFO and ASA alone.

Table 3. Total numbers of other embolic sources in addition to patent foramen ovale or combined patent foramen ovale and atrial septal aneurysm

	All patients (n=58)	Younger (n=15)	Older (n=43)	P value
Total numbers of other embolic sources in addition to PFO or combined PFO and ASA				0.017
0(%)	26(44.8)	12(80.0)	14(32.6)	-
1(%)	19(32.8)	2(13.3)	17(39.5)	-
2(%)	12(20.7)	1(6.7)	11(25.6)	-
3(%)	1(1.7)	0(0)	1(2.3)	-

PFO: patent foramen ovale; ASA: atrial septal aneurysm.

Discussion

TEE is superior to transthoracic echocardiography for identifying intracardiac abnormalities [4]. It is especially useful for identifying abnormal structures in detail, such as PFO and ASA, or other intracardiac embolic sources, such as LAAF, Chiari networks, and aortic valve calcification. A previous study has already shown the association between the presence of PFO and cryptogenic stroke in both older and younger patients [5]. However, it did not clearly evaluate other causes of ESUS except for PFO and ASA. Moreover, no other previous study has clearly assessed and classified the distribution of causes according to the ESUS criteria [1]. The present study utilized TEE to identify other causes of ESUS according to the ESUS criteria.

The prevalence of PFO on echocardiographic and autopsy studies in the healthy adult population is approximately 20%–25% [6–8]. Furthermore, approximately 40%–60% of cases of stroke with paradoxical embolism in young people are associated with PFO [8, 9, 19]. Notably, our study showed a higher incidence of PFO in ESUS patients compared with previous studies, which may be attributed to our definition of PFO, i.e., the presence of at least one microbubble in the left atrium within three cardiac cycles after opacification of the right atrium using agitated saline contrast microbubbles [9], regardless of the number of microbubbles. In addition, a previous study showed a positive relationship between the size of the shunt and the risk of stroke [10]. Some authors have indicated that PFO size can be defined by the

number of microbubbles, where 3–10 microbubbles is a small shunt, 1–30 is a moderate shunt, and >30 is a large shunt [11]. Other previous studies have identified that the morphological or functional characteristics of PFO are associated with paradoxical embolic stroke [12, 13]. In our study, these elements of PFO were not evaluated; however, we evaluated the frequency of ASA and found that it was anatomically related to PFO. The coexistence of PFO and ASA is a stronger risk factor for stroke than either source by itself [14]. Our study demonstrated that the frequency of PFO or combined PFO and ASA without other cardioembolic sources was 80% and 32.6% in younger and older ESUS patients, respectively.

Three previous trials, the CLOSURE-1 trial (Evaluation of the STARFlex Septal Closure System in Patients with a Stroke and/or Transient ischemic Attack due to Presumed Paradoxical Embolism through a PFO) [15], the RESPECT trial (Randomized Evaluation of Recurrent Stroke Comparing PFO Closure to Established Current Standard of Care Treatment) [16] and the PC trial (Randomized Clinical Trial Comparing the Efficacy of Percutaneous Closure of Patent Foramen Ovale With Medical Treatment in Patients With Cryptogenic Embolism) [17] did not show a superiority for PFO closure over medical therapy in patients with cryptogenic stroke. However, more recent trials showed that PFO closure is effective in preventing recurrent stroke [2, 3, 18]. These trials reported that the rates of recurrent stroke in younger (18–60 years) patients were significantly lower with closure of the PFO plus antiplatelet therapy than with antiplatelet therapy

alone. However, the clinical benefit of PFO closure for preventing recurrent stroke in older patients with stroke-related PFO has not been adequately evaluated. We believe that PFO closure in older patients might be considered if no causes of embolic source other than PFO and ASA are detected in patients with ESUS who undergo routine diagnostic assessment with additional TEE. Further study of larger numbers of ESUS patients is necessary to confirm our results.

Our study has several limitations. First, this was a single-center, retrospective study, which potentially introduces selection bias. Second, only a small number of patients were analyzed. Third, undetected causes, such as subclinical paroxysmal atrial fibrillation, may have existed in the study population. All patients of this study underwent cardiac monitoring for ≥ 24 h with automated rhythm detection and none had any atrial high rate episodes up until discharge. This is insufficient monitoring, especially in older patients because the current recommendation is 2-4 weeks of ECG monitoring. Fourth, we did not have follow up on the older patients who had PFO closure. It is unknown whether PFO closure of older ESUS patients related PFO is efficacy same as younger. However, we believe that our study population reflects a real world unselected population of patients with ESUS.

References

- Hart RG, Diener HC, Coutts SB, Easton JD, Granger CB, O'Donnell MJ, et al. Embolic strokes of undetermined source: the case for a new clinical construct. *Lancet Neurol.* 2014;13:429-438. DOI: [10.1016/S1474-4422\(13\)70310-7](https://doi.org/10.1016/S1474-4422(13)70310-7)
- Sondergaard L, Kasner SE, Rhodes JF, Andersen G, Iversen HK, Nielsen-Kudsk JE, et al. Patent foramen ovale closure or antiplatelet therapy for cryptogenic stroke. *N Engl J Med.* 2017;377:1033-1042. DOI: [10.1056/NEJMoa1707404](https://doi.org/10.1056/NEJMoa1707404)
- Saver JL, Carroll JD, Thaler DE, Smalling RW, MacDonald LA, Marks DS, et al. Long-Term outcomes of patent foramen ovale closure or medical therapy after stroke. *N Engl J Med.* 2017;377:1022-1032. DOI: [10.1056/NEJMoa1610057](https://doi.org/10.1056/NEJMoa1610057)
- Pearson AC, Labovitz AJ, Tatini S, Gomez CR. Superiority of transesophageal echocardiography in detecting cardiac source of embolism in patients with cerebral ischemia of uncertain etiology. *J Am Coll Cardiol.* 1991;17:66-72. DOI: [10.1016/0735-1097\(91\)90705-E](https://doi.org/10.1016/0735-1097(91)90705-E)
- Handke M, Harloff A, Olschewski M, Hetzel A, Geibel A. Patent foramen ovale and cryptogenic stroke in older patients. *N Engl J Med.* 2007;357:2262-2268. DOI: [10.1056/NEJMoa071422](https://doi.org/10.1056/NEJMoa071422)
- Meissner I, Whisnant JP, Khandheria BK, Spittell PC, O'Fallon WM, Pascoe RD, et al. Prevalence of potential risk factors for stroke assessed by transesophageal echocardiography and carotid ultrasonography: the SPARC study. *Stroke Prevention: Assessment of Risk in a Community.* Mayo Clin Proc. 1999;74:862-869. DOI: [10.4065/74.9.862](https://doi.org/10.4065/74.9.862)
- Schneider B, Zienkiewicz T, Jansen V, Hofmann T, Noltenius H, Meinertz T. Diagnosis of patent foramen ovale by transesophageal echocardiography and correlation with autopsy findings. *Am J Cardiol.* 1996;77:1202-1209. DOI: [10.1016/S0002-9149\(96\)00163-4](https://doi.org/10.1016/S0002-9149(96)00163-4)
- Lechat P, Mas JL, Lascault G, Loron P, Theard M, Klimczak M, et al. Prevalence of patent foramen ovale in patients with stroke. *N Engl J Med.* 1988;318:1148-1152. DOI: [10.1056/NEJM198805053181802](https://doi.org/10.1056/NEJM198805053181802)
- Webster MW, Chancellor AM, Smith HJ, Swift DL, Sharpe DN, Bass NM, et al. Patent foramen ovale in young stroke patients. *Lancet.* 1988;2:11-12. DOI: [10.1016/S0140-6736\(88\)92944-3](https://doi.org/10.1016/S0140-6736(88)92944-3)
- Stone DA, Godard J, Corretti MC, Kittner SJ, Sample C, Price TR, et al. Patent foramen ovale: association between the degree of shunt by contrast transesophageal echocardiography and the risk of future ischemic neurologic events. *Am Heart J.* 1996;131:158-161. DOI: [10.1016/S0002-8703\(96\)90065-4](https://doi.org/10.1016/S0002-8703(96)90065-4)
- Mas JL, Arquizan C, Lamy C, Zuber M, Cabanes L, Derumeaux G, et al. Recurrent cerebrovascular events associated with patent foramen ovale, atrial septal aneurysm, or both. *N Engl J Med.* 2001;345:1740-1746. DOI: [10.1056/NEJMoa011503](https://doi.org/10.1056/NEJMoa011503)
- Hausmann D, Mugge A, Daniel WG. Identification of patent foramen ovale permitting paradoxical embolism. *J Am Coll Cardiol.* 1995;26:1030-1038. DOI: [10.1016/0735-1097\(95\)00288-9](https://doi.org/10.1016/0735-1097(95)00288-9)

Conclusion

The embolic sources of ESUS were similar between younger and older patients except for aortic arch atherosclerotic plaques. However, the total number of embolic sources was significantly higher in older patients. Therefore, it is difficult to determine a distinct single cause of stroke in older ESUS patients. Both younger patients and a small percentage of older patients have a risk of paradoxical embolism only, such as PFO or both PFO and ASA. Routine diagnostic assessment with additional TEE could help clarify the causes of ESUS.

Conflict of Interest

The authors have no conflict of interest relevant to this publication.

[Comment on this Article or Ask a Question](#)

13. De Castro SD, Cartoni D, Fiorelli M, Rasura M, Anzini A, Zanette EM, et al. Morphological and functional characteristics of patent foramen ovale and their embolic implications. *Stroke*. 2000;31:2407-2413. DOI: <https://doi.org/10.1161/01.STR.31.10.2407>
14. Overell JR, Bone I, Lees KR. Interatrial septal abnormalities and stroke: a meta-analysis of case-control studies. *Neurology*. 2000;55:1172-1179. DOI: [10.1212/WNL.55.8.1172](https://doi.org/10.1212/WNL.55.8.1172)
15. Furlan AJ, Reisman M, Massaro J, Mauri L, Adams H, Albers GW, et al. Closure or medical therapy for cryptogenic stroke with patent foramen ovale. *N Engl J Med*. 2012;366:991-999. DOI: [10.1056/NEJMoa1009639](https://doi.org/10.1056/NEJMoa1009639)
16. Carroll JD, Saver JL, Thaler DE, Smalling RW, Berry S, MacDonald LA, et al. Closure of patent foramen ovale versus medical therapy after cryptogenic stroke. *N Engl J Med*. 2013;368:1092-1100. DOI: [10.1056/NEJMoa1301440](https://doi.org/10.1056/NEJMoa1301440)
17. Meier B, Kalesan B, Mattle HP, Khattab AA, Hildick-Smith D, Dudek D, et al. Percutaneous Closure of Patent Foramen Ovale in Cryptogenic Embolism. *N Engl J Med*. 2013;368:1083-1091. DOI: [10.1056/NEJMoa1211716](https://doi.org/10.1056/NEJMoa1211716)
18. Mas JL, Derumeaux G, Guillon B, Massardier E, Hosseini H, Mechtouff L, et al. Patent foramen ovale closure or anticoagulation vs. antiplatelets after stroke. *N Engl J Med*. 2017;377:1011-1021. DOI: [10.1056/NEJMoa1705915](https://doi.org/10.1056/NEJMoa1705915)
19. West BH, Nouredin N, Mamzhi Y, Low CG, Coluzzi AC, Shih EJ, et al. Frequency of Patent Foramen Ovale and Migraine in Patients With Cryptogenic Stroke. *Stroke*. 2018;49:1123-1128. DOI: [10.1161/STROKEAHA.117.020160](https://doi.org/10.1161/STROKEAHA.117.020160)

Cite this article as: Takafuji H, Hosokawa S, Ogura R, Hiasa Y. Difference Among Embolic Sources Between Younger and Older Patients With Stroke of Undetermined Source on Routine Diagnostic Assessment Including Transesophageal Echocardiography. *Structural Heart Disease*. 2019;5(5):206-212. DOI: <https://doi.org/10.12945/j.jshd.2019.034.18>

Assessment of the Dynamism of the Left Atrial Appendage Dimensions: A Computer Tomographic Analysis

Mohamed Marwan, MD*, Amina Vaillant, Fabian Ammon, MD, Daniel Bittner, MD, Michaela Hell, MD, Stephan Achenbach, MD

Department of Cardiology, University of Erlangen-Nuremberg, Erlangen, Germany

Abstract

Background: Device sizing prior to left atrial appendage (LAA) closure is currently primarily based on transesophageal echocardiographic as well as invasive angiographic measurements, and can be challenging due to the complex and highly variable anatomy of the LAA. Computerized tomography (CT) is a 3-dimensional imaging modality that is increasingly being used for planning structural heart disease interventions. We assessed the variability of the measurements of the LAA ostium in patients with sinus rhythm and atrial fibrillation referred for CT angiography.

Methods: 101 consecutive patients with available retrospective spiral acquisitions as well as multiphase reconstructions between 0 to 90% of the peak R-wave to R-wave were included in this analysis. All acquisitions were performed using a third generation dual source system (Somatom Force, Siemens Healthineers, Forchheim, Germany). Data sets were transferred to dedicated Software (Ziostation2, Ziosoft Inc., Tokyo, Japan) which allows dynamic evaluation of the LAA ostium through the different phases of the cardiac cycle. Multiplanar reconstructions were aligned with the plane of the LAA ostium and measurements were performed in a cross-sectional plane orthogonal to the long axis of the LAA at the level of the left circumflex coronary artery. Four measurements were performed: area, circumference, area-derived diameter ($\sqrt{[\text{area}/\pi] \times 2}$) and circumference-derived (perimeter/ π). Furthermore assessment of the length of the LAA was assessed in all patients.

Results: Out of 101 patients (mean age 81 ± 8 years, 61% males), 48 patients were in sinus rhythm at time of acquisition and 53 patients were in atrial fibrillation. The mean area of the LAA ostium as well as perimeter were significantly larger in AF patients compared to SR patients (464 ± 153 vs. 359 ± 131 mm² and 78 ± 12 mm vs. 69 ± 12 mm for AF vs SR patients, respectively, $p=0.001$). Consequently the area derived diameter as well as perimeter derived diameter were consequently significantly larger in AF vs. SR patients (24 ± 4 mm vs. 21 ± 4 mm and 25 ± 4 vs. 22 ± 4 mm for area-derived vs. perimeter-derived diameter, respectively, $p<0.001$). The percentage difference between maximal and minimal LAA dimensions were significantly higher for sinus rhythm patients compared to atrial fibrillation [88% (IQR 60; 147%) vs. 21% (IQR 13; 42%), respectively, $p<0.001$] for median percentage area change and 34% vs. 10% for median percentage perimeter change (IQR 25; 52 vs. 7; 18%, respectively, $p<0.001$).

For atrial fibrillation patients, the largest LAA dimensions (area, perimeter, area-derived and perimeter-derived diameters) was measured at an average of 40% of the peak R-wave to R-wave whereas for sinus rhythm patients, the maximal LAA dimensions were measured at an average of 46% of the peak R-wave to R-wave ($p>0.05$). The mean length of the LAA was significantly larger in AF patients compared to SR patients (19.5 mm vs. 17 mm for AF vs SR patients, $p=0.04$) and the median percentage change in length was significantly higher in SR vs. AF (32% [IQR 19; 61%] vs. 13% [IQR 9; 19%] for SR vs. AF patients)



Conclusions: Dimensions of the left atrial appendage ostium vary significantly within different time points in cardiac cycle. These changes are more pronounced in patients in sinus rhythm compared to patients in atrial fibrillation which might impact sizing if CT is used for procedural planning prior to interventional closure of the LAA. According to our data, to identify maximal LAA dimensions, CT imaging for the purpose of LAA occlusion should be targeted in atrial diastole (40-50% of the peak R-wave to R-wave).

Copyright © 2019 Science International Corp.

Key Words

LAA • Closure • Sizing • CT

Introduction

The association between atrial fibrillation and ischemic cerebrovascular events has been established in numerous prospective studies [1]. Oral anticoagulation is currently the therapy of choice to prevent thromboembolic complications in patients with atrial fibrillation [2]. For patients at high risk for bleeding on anticoagulation therapy, percutaneous mechanical occlusion of the left atrial appendage (LAA) has emerged as an effective approach for stroke prevention [1]. Correct sizing is crucial for successful and safe implantation of the LAA occluder as well as for achieving desired outcomes following interventional closure. Clinically significant complications, including hemodynamically significant pericardial effusion or procedure-related stroke, are reported in up to 4% of cases [3]. Device sizing prior to left atrial appendage (LAA) closure is currently primarily based on transthoracic echocardiographic as well as invasive angiographic measurements, and can be challenging due to the complex and highly variable anatomy of the LAA. Moreover, apart from the complexity of the left atrial appendage anatomy, the LAA has the ability to contract and the dimensions of the LAA-ostium can change variably during the cardiac cycle leading to differences in sizing strategies. CT is a 3-dimensional imaging modality that is increasingly being used for planning structural heart disease interventions [4-11]. Next to its high and isotropic spatial resolution, CT has the advantage of allowing imaging throughout the entire cardiac cycle in arbitrary orientations.

Using multiphase computed tomography, we assessed the variability of the LAA dimensions in patients with sinus rhythm and atrial fibrillation throughout the cardiac cycle.

Material and Methods

Study design and patient population

This is a single center, retrospective study. Consecutive CT data sets of 101 patients referred for assessment prior to or following transcatheter aortic valve replacement were included in this analysis.

DSCCT data acquisition and image reconstruction

CT data sets were acquired with a third generation dual source CT system (Somatom Force, Siemens Healthineers, Forchheim, Germany) using spiral acquisition with retrospectively ECG-gated reconstruction, with a scan range extending from the pulmonary artery bifurcation to the caudal aspect of the heart. Scan parameters were as follows: tube voltage 100 kV, tube current time product 500 mAs, collimation 2x192x0.6 mm and rotation time 250ms. ECG dose modulation was used with full radiation exposure between 10-70% of the R-wave to R-wave interval and a dose reduction to 20% outside this window. To assess contrast agent transit time, 10ml of contrast agent (Ultravist 370®, Bayer vital, Leverkusen, Germany) was used. For CT angiography, 50 ml at a flow rate of 5ml/sec, followed by a 50 ml saline chaser at the same flow rate was injected.

For each patient, a multiphase reconstruction in 10% increments of the cardiac cycle was rendered using a small field of view data set to allow for 4-dimensional assessment of the left atrial appendage. All reconstructions were rendered using a medium soft convolution kernel (Siemens Bv40) with a slice thickness of 0.75 mm and slice increment of 0.5 mm and iterative reconstruction (Admire®, Siemens Healthineers, Forchheim, Germany) at a strength level of 2.

CT analysis of left atrial appendage

For primary analysis, multiphase reconstructions were transferred to a dedicated workstation (Ziostation2, Ziosoft Inc., Tokyo, Japan). The plane of the left atrial appendage ostium was defined as a plane connecting the upper left pulmonary vein superi-

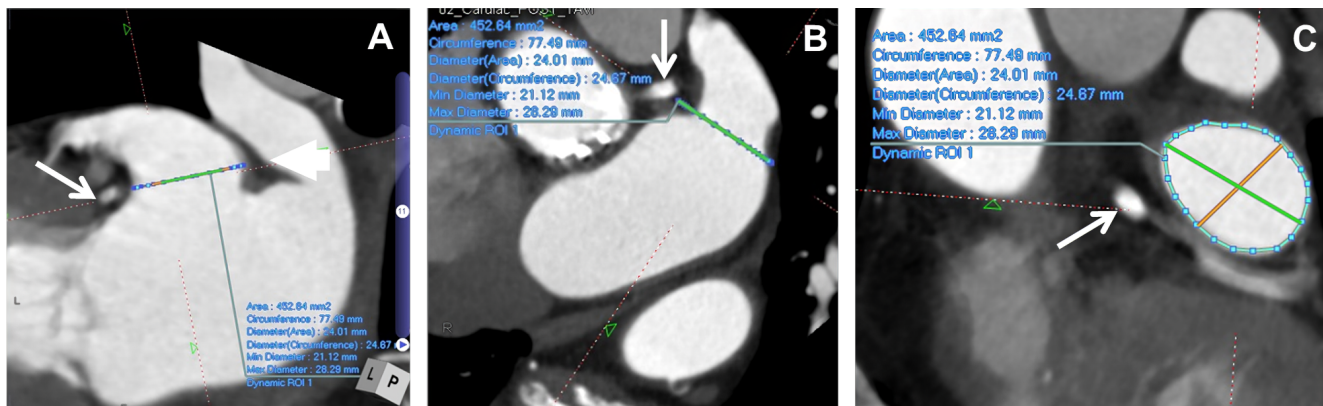


Figure 1. Panel A & B. Multiplanar reconstruction of the left atrial appendage (LAA) showing the plane of the ostium (dotted line). The plane of the ostium is orthogonal to the long axis of the LAA and extends from the upper pulmonary vein ridge (thick arrow) to the plane of the left circumflex coronary artery (thin arrow). Panel C. Tracing of the LAA ostial plane in cross-section..

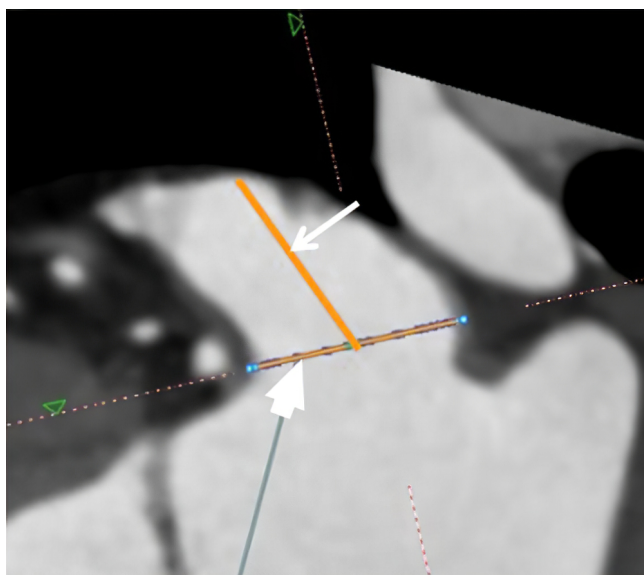


Figure 2. Multiplanar reconstruction of the left atrial appendage (LAA) showing the measurement of the length of the LAA (thin arrow). The plane of the LAA ostium is marked by the thick arrow.

only and the connection of the left atrium and LAA inferiorly at the level of the left circumflex coronary artery. Moreover this plane was adjusted strictly orthogonal to the long axis of the LAA. The orifice of the LAA was then manually traced with at least 18 points across its contour (Figure 1) and an automated algorithm automatically provided the area, circumference, maximum and minimal diameters as well as an area-derived diameter ($\sqrt{[\text{area}/\pi]} \times 2$) and a circumference-derived (perimeter/ π) of the traced contour.

The manual tracing of the plane of the LAA was only performed at one time point in the cardiac cycle and then automatically propagated by the software to all other phases. In every phase the tracing of the LAA ostial plane was visually verified and, if required corrected for possible errors according to the discretion of the observer. Furthermore, for each LAA the length was measured defined as the distance from the apex of the LAA to the plane of the ostium or in case of LAA with significant bends as the distance from the plane of the LAA ostium to the first bend. (Figure 2) The dimensions of the LAA ostium were compared between 48 patients with sinus rhythm and 53 in atrial fibrillation. Moreover the percentage change in dimensions (area, perimeter, area-derived diameter, perimeter derived diameter and length) defined as the percentage difference between the smallest measurement and the largest measurement were compared between both groups.

Statistical analyses

Continuous data are presented as mean \pm standard deviation or median and interquartile range. Categorical variables are shown in proportions. Mean values were compared using t-test for normally distributed data and Mann-Whitney for data with non-normal distribution.

All statistical analyses were performed using IBM® (New York) SPSS® Statistics (version 21.0).

Results

Study population

101 patients were included in this analysis (mean age 81 ± 8 years, 61% males). Patients were divided in two groups: 48 patients in sinus rhythm (SR) and 53 patients in atrial fibrillation (either paroxysmal or persistent). All patients in the atrial fibrillation (AF) group were in AF during the CT acquisition. Baseline characteristics are shown in Table 1. Mean heart rate during the CT exam was 62 ± 9 bpm for patients with sinus rhythms vs. 69 ± 8 bpm in patients in atrial fibrillation ($p = n.s.$).

Left atrial appendage ostium dimensions

The mean area of the LAA ostium as well as perimeter were significantly larger in AF patients compared to SR patients (464 ± 153 vs. 359 ± 131 mm² and 78 ± 12 mm vs. 69 ± 12 mm for AF vs SR patients, respectively, $p = 0.001$). Consequently the area derived diameter as well as perimeter derived diameter were consequently significantly larger in AF vs. SR patients (24 ± 4 mm vs. 21 ± 4 mm and 25 ± 4 vs. 22 ± 4 mm for area-derived vs. perimeter-derived diameter, respectively, $p < 0.001$). (Table 2 and 3) The percentage difference between maximal and minimal LAA dimensions were significantly higher for sinus rhythm patients compared to atrial fibrillation [88% (IQR 60; 147%) vs. 21% (IQR 13; 42%), respectively, $p < 0.001$] for median percentage area change and 34% vs. 10% for median percentage perimeter change (IQR 25;52 vs. 7;18%, respectively, $p < 0.001$) (Figure 3).

For atrial fibrillation patients, the largest LAA dimensions (area, perimeter, area-derived and perimeter-derived diameters) was measured at an average of 40% of the peak R-wave to R-wave whereas for sinus rhythm patients, the maximal LAA dimensions were measured at an average of 46% of the peak R-wave to R-wave ($p > 0.05$).

Left atrial appendage length

The mean length of the LAA was significantly larger in AF patients compared to SR patients (19.5 mm vs. 17 mm for AF vs SR patients, $p = 0.04$) and the median percentage change in length was significantly higher in SR vs. AF (32% [IQR 19; 61%] vs. 13% [IQR 9; 19%] for SR vs. AF patients)

Table 1: Baseline clinical characteristics.

	Sinus rhythm	AF	P-Value
Patients (n)	48	53	
Male Gender (%)	30 (62)	32 (60)	0.84
Age in years (mean \pm SD)	80 ± 8	82 ± 6	0.52
Coronary artery disease (%)	28 (58)	38 (72)	0.21
Cardiovascular Risk Factors			
Dyslipidemia (%)	28 (58)	27 (51)	0.55
Hypertension (%)	36 (75)	45 (85)	0.23
Diabetes mellitus (%)	11 (23)	16 (30)	0.50
Smoking			0.74
Ex-Smoker	3(6)	4(8)	
Current Smoker	2/4	4(8)	
Positive Family History (%)	3 (6)	4 (8)	1.00

Discussion

In this retrospective analysis, we demonstrate a significant change in LAA ostial dimensions through the cardiac cycle with maximum measurements for both perimeter as well as area measurements at 40-50% of the electrocardiographic peak R- wave to R-wave corresponding to atrial diastole. This dynamism is, as intuitively assumed more pronounced for patients in sinus rhythm – due to the contractile function of the left atrial appendage - compared to patients in atrial fibrillation (median percentage area and perimeter change 88% and 34% vs. 21% and 10% for SR vs. AF patients, respectively). Nevertheless, AF patients – a subset that might come in question for percutaneous LAA occlusion – still demonstrate a certain degree of dynamism of the LAA ostium dimensions potentially influencing sizing strategies for different LAA occluders available on market.

So far, several studies have reported on the use of 3-dimensional imaging (specifically CT imaging) prior to LAA interventions. In a large single center registry of 73 patients, Rajwani et al. reported a favorable outcome for LAA occlusion procedures using routine incorporation of CT data for pre-procedural sizing [12].

Table 2: Area measurement of LAA ostium through the cardiac cycle.

LAA Area	Sinus rhythm	AF	P-value
Mean \pm SD (mm ²)	359 \pm 131	464 \pm 153	0.001
Median (mm ²)	378 \pm 140	468 \pm 150	0.002
Minimum (mm ²)	233 \pm 108	406 \pm 169	< 0.001
Maximum (mm ²)	440 \pm 150	517 \pm 154	0.025
Percentage Difference % Median (IQR)	88 (60;147)	21 (13;42)	< 0.001
Time point maximum area (% R-wave to R-wave peak, mean \pm SD)	46 \pm 13	40 \pm 15	0.16

In their cohort - albeit in a retrospective fashion - , CT assessment altered device selection in more than half of the cases, compared to standard transoesophageal echocardiography (TEE). In this study, CT acquisitions were performed using high-pitch spiral acquisitions which per standard are set to be triggered at 60% of the peak R-wave to R-wave. However in the setting of atrial fibrillation, a clear knowledge of the exact time trigger of the acquisition remains questionable for this CT acquisition mode. Along the same line, in a cohort of 53 patients examined by Wang et al., device selection using CT imaging prior to LAA occlusion showed 100% accuracy, whereas the use of maximal LAA ostial diameters whether in 2D-TEE or 3D-TEE would have resulted in incorrect device selection in 62% and 53%, respectively [13]. In this study, sizing of the LAA was performed using ventricular systolic phases corresponding to the maximal diastolic atrial filling. In a more recent study by Eng et al., a small cohort (a total of 24 patients) was prospectively randomized to CT vs. TEE guidance prior to LAA occlusion [14]. The authors demonstrated a better device selection as well as procedural efficiency for the CT arm compared to the TEE arm. In fact, in this small cohort, the accuracy of first device selection was 92% compared to 27% for CT vs. TEE. Although CT acquisitions were performed using retrospective ECG-triggering, no clear mention of the exact time point of LAA sizing

Table 3: Perimeter measurement of LAA ostium through the cardiac cycle.

LAA Perimeter	Sinus rhythm	AF	P-value
Mean \pm SD (mm)	69 \pm 12	78 \pm 12	0.001
Median (mm)	72 \pm 13	79 \pm 12	0.007
Minimum (mm, mean \pm SD)	56 \pm 13	73 \pm 15	< 0.001
Maximum (mm, mean \pm SD)	77 \pm 13	83 \pm 11	0.031
Percentage Difference % Median (IQR)	34 (25;52)	10 (7;18)	< 0.001
Time point maximum Perimeter (% R-wave to R-wave peak, mean \pm SD)	47 \pm 15	41 \pm 19	0.23

was reported. Furthermore, in a cohort of 36 patients examined using CT as well as 2-dimensional TEE, Goitein et al. reported a better prediction of device sizing prior to percutaneous LAA occlusion using perimeter assessment of LAA ostium in CT compared to diameter measurements in TEE [15]. In their cohort, acquisitions were performed in ventricular systole at 30-40% of the cardiac cycle.

Beyond 3-dimensional assessment of the LAA using CT imaging, few studies have recently reported the feasibility and usefulness of CT-based 3D printing for assessment of the LAA prior to percutaneous closure [16-18]. Using this modern technology, Hell et al. could demonstrate - in a small cohort of 22 patients treated with the Watchman® device - the additive value of CT-based 3D printing compared to anatomical CT 3-dimensional information for device selection prior to percutaneous closure [16].

Moreover, Hozawa et al. recently compared LAA volume and dimensions in 60 patients with normal sinus rhythm compared to patients with paroxysmal atrial fibrillation [19]. In their cohort, CT imaging was performed at 75% of the peak R-wave to R-wave in patients with sinus rhythm (ventricular diastolic phase) whereas for patients with paroxysmal AF, retrospective CT acquisitions along the entire cardiac cycle were available. However, for the purpose of comparison, LAA dimensions were compared only in

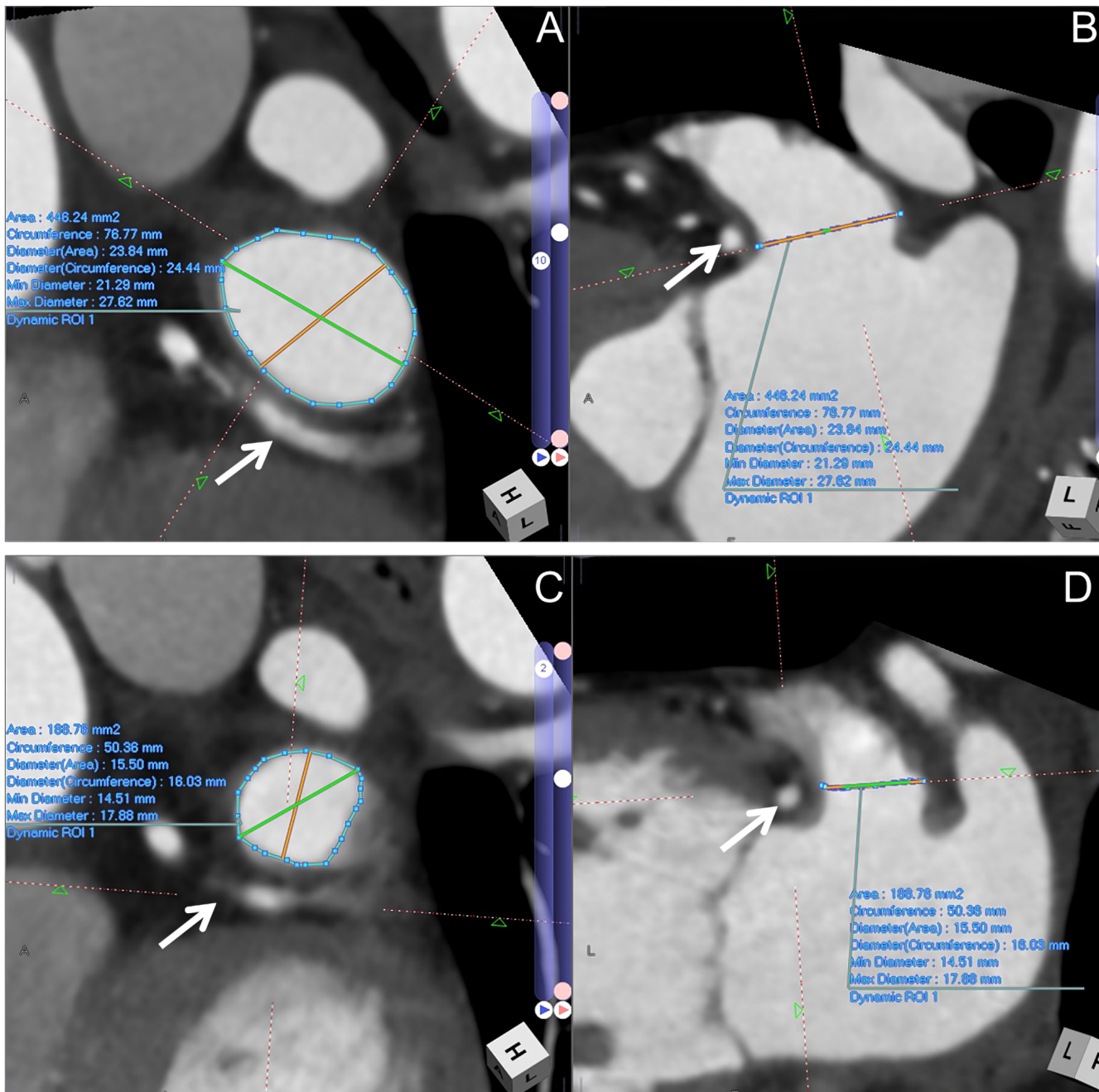


Figure 3. Computed tomography of a 70-year-old patient in sinus rhythm. *Panels A and B* show multiplanar reconstructions of the left atrial appendage (LAA) at 45% of the peak R-wave to R-wave. *Panel A.* Tracing of the LAA ostium showing an area of 446 mm². *Panel B.* plane of the LAA ostium. The **arrows** mark the left circumflex coronary artery. *Panels C and D* show multiplanar reconstructions of the same patient at 5% of the peak R-wave to R-wave with significantly smaller LAA dimensions. *Panel C.* Tracing of the LAA ostium showing an area of 188 mm². *Panel D.* plane of the LAA ostium.

ventricular diastolic phases for both sinus rhythm and atrial fibrillation patients (75% of the peak R-wave to R-wave). Similar to our observation – albeit with com-

parisons only in ventricular diastolic phases- the authors report significantly larger dimensions of LAA-orifice as well as LAA volume in AF patients compared

to sinus rhythm patients. Interestingly, the authors addressed a further challenging aspect of LAA assessment which is the definition of the LAA ostial plane. In their analysis, three planes were proposed for assessment of the LAA orifice. Due to the lack of anatomical boundaries between the left atrial cavity and the LAA, it still remains challenging to uniformly define the plane of the ostium. So far, the most commonly used plane for defining the LAA ostium is a plane joining the pulmonary vein ridge superiorly and the junction between the LA and the LAA inferiorly at the plane the left circumflex coronary artery. Of Interest, using a similarly defined plane in their cohort and ours, Hozawa et al. could only demonstrate a trend towards larger LAA ostial dimensions in AF patients compared to sinus rhythm, however these differences did not reach statistical significance. These differences could be probably explained by the difference in cohort size on one side, and more importantly due to the mere ventricular diastolic phase assessment in their cohort on the other side.

In light of our findings, it appears of relevant importance to plan the time of CT acquisition to the time point of maximal LAA dimensions for optimal device sizing and consequently optimal sealing of the LAA. However, we examined a cohort of patients referred for CT imaging in the context of transcatheter aortic valve replacement, as these patients were – per institutional protocol - examined using retrospective acquisition and hence multiphase assessment of LAA dimensions at different time points of the cardiac cycle was possible. In so far, whether implementing CT maximal LAA dimensions for device sizing outside this selected cohort would affect intra-procedural success as well as complications remains unclear and need to be further assessed in a prospective cohort referred for percutaneous LAA occlusion.

References

1. Kirchhof P, Benussi S, Kotecha D, Ahlsson A, Atar D, Casadei B, et al. 2016 ESC Guidelines for the management of atrial fibrillation developed in collaboration with EACTS. *Eur Heart J*. 2016;37:2893-2962. DOI: [10.1093/eurheartj/ehw210](https://doi.org/10.1093/eurheartj/ehw210)
2. Granger CB, Armaganijan LV. Newer oral anticoagulants should be used as first-line agents to prevent thromboembolism in patients with atrial fibrillation and risk factors for stroke or thromboembolism. *Circulation*. 2012;125:159-164. DOI: [10.1161/CIRCULATIONAHA.111.031146](https://doi.org/10.1161/CIRCULATIONAHA.111.031146)
3. Holmes Jr DR, Kar S, Price MJ, Whisenant B, Sievert H, Doshi SK, et al. Prospective randomized evaluation of the Watchman Left Atrial Appendage Closure device in patients with atrial fibrillation versus long-term warfarin therapy: the PREVAIL trial. *J Am Coll Cardiol*. 2014;64:1-12. DOI: [10.1016/j.jacc.2014.04.029](https://doi.org/10.1016/j.jacc.2014.04.029)
4. Achenbach S, Delgado V, Hausleiter J, Schoenhagen P, Min, JK, Leipzig JA. SCCT expert consensus document on computed tomography imaging before transcatheter aortic valve implantation (TAVI)/transcatheter aortic valve replacement (TAVR). *J Cardiovasc Comput Tomogr*. 2012;6:366-380. DOI: [10.1016/j.jcct.2012.11.002](https://doi.org/10.1016/j.jcct.2012.11.002)
5. Blanke P, Dvir D, Cheung A, Levine RA,

Several limitations in this study need to be acknowledged. First, our patient cohort included a relatively small cohort referred for CT imaging prior to transcatheter aortic valve replacement. Furthermore CT measurements were performed by a single observer once so intra- and inter-observer differences could not be reported. However, our data shed light on the importance of careful timing of CT acquisitions in the context of LAA imaging prior to interventional closure. The currently available literature is somehow heterogeneous as far as CT acquisition protocols prior to LAA occlusion are concerned. Especially with the expected increase in CT imaging in this context, standardized acquisition protocols as well as reporting algorithms need to be developed to allow for standardized reporting. According to our data, to identify maximal LAA dimensions, CT imaging for the purpose of LAA occlusion should be targeted in atrial diastole (40-50% of the peak R-wave to R-wave).

Acknowledgment

We would like to express our sincere thanks to Mr. Tsuyoshi Nagata from Ziosoft for his help and assistance in the processing of the CT data sets as well as his continuous support with data analysis. The present work was carried out by Amina Vaillant to meet the requirements for obtaining the degree “Dr. med.” at Friedrich-Alexander-University Erlangen-Nürnberg (FAU).

Conflict of Interest

Mohamed Marwan has received speaker honoraria from Siemens Healthcare and Edwards Lifesciences.

Comment on this Article or Ask a Question

- Thompson C, Webb JG, et al. Mitral Annular Evaluation With CT in the Context of Transcatheter Mitral Valve Replacement. *JACC Cardiovasc Imaging*. 2015;8:612-615. DOI: [10.1016/j.jcmg.2014.07.028](https://doi.org/10.1016/j.jcmg.2014.07.028)
6. Blanke P, Naoum C, Webb JG, Dvir D, Hahn RT, Grayburn P, et al. Multimodality Imaging in the Context of Transcatheter Mitral Valve Replacement: Establishing Consensus Among Modalities and Disciplines. *JACC Cardiovasc Imaging*. 2015;8:1191-1208. DOI: [10.1016/j.jcmg.2015.08.004](https://doi.org/10.1016/j.jcmg.2015.08.004)
 7. Blanke P, Park JK, Grayburn P, Naoum C, Ong K, Kohli K, et al. Left ventricular access point determination for a coaxial approach to the mitral annular landing zone in transcatheter mitral valve replacement. *J Cardiovasc Comput Tomogr*. 2017;11:281-287. DOI: [10.1016/j.jcct.2017.04.002](https://doi.org/10.1016/j.jcct.2017.04.002)
 8. Ismail TF, Panikker S, Markides V, Foran JP, Padley S, Rubens MB, et al. CT imaging for left atrial appendage closure: a review and pictorial essay. *J Cardiovasc Comput Tomogr*. 2015;9:89-102. DOI: [10.1016/j.jcct.2015.01.011](https://doi.org/10.1016/j.jcct.2015.01.011)
 9. Korsholm K, Jensen JM, Nielsen-Kudsk JE. Cardiac Computed Tomography for Left Atrial Appendage Occlusion: Acquisition, Analysis, Advantages, and Limitations. *Interv Cardiol Clin*. 2018;7:229-242. DOI: [10.1016/j.iccl.2017.12.004](https://doi.org/10.1016/j.iccl.2017.12.004)
 10. Lazoura O, Ismail TF, Pavitt C, Lindsay A, Sriharan M, Rubens M, et al. A low-dose, dual-phase cardiovascular CT protocol to assess left atrial appendage anatomy and exclude thrombus prior to left atrial intervention. *Int J Cardiovasc Imaging*. 2016;32:347-354. DOI: [10.1007/s10554-015-0776-x](https://doi.org/10.1007/s10554-015-0776-x)
 11. Naoum C, Blanke P, Cavalcante JL, Leipsic J. Cardiac Computed Tomography and Magnetic Resonance Imaging in the Evaluation of Mitral and Tricuspid Valve Disease: Implications for Transcatheter Interventions. *Circ Cardiovasc Imaging*. 2017;10:e005331. DOI: [10.1161/CIRCIMAGING.116.005331](https://doi.org/10.1161/CIRCIMAGING.116.005331)
 12. Rajwani A, Nelson AJ, Shirazi MG, Disney PJS, Teo KSL, Wong DTL, et al. CT sizing for left atrial appendage closure is associated with favourable outcomes for procedural safety. *Eur Heart J Cardiovasc Imaging*. 2017;18:1361-1368. DOI: [10.1093/ehjci/jew212](https://doi.org/10.1093/ehjci/jew212)
 13. Wang DD, Eng M, Kupsy D, Myers E, Forbes M, Rahman M, et al. Application of 3-Dimensional Computed Tomographic Image Guidance to WATCHMAN Implantation and Impact on Early Operator Learning Curve: Single-Center Experience. *JACC Cardiovasc Interv*. 2016;9:2329-2340. DOI: [10.1016/j.jcin.2016.07.038](https://doi.org/10.1016/j.jcin.2016.07.038)
 14. Eng MH, Wang DD, Greenbaum AB, Gheewala N, Kupsy D, Aka T, et al. Prospective, randomized comparison of 3-dimensional computed tomography guidance versus TEE data for left atrial appendage occlusion (PRO3DLAAO). *Catheter Cardiovasc Interv*. 2018;1;92:401-407. DOI: [10.1002/ccd.27514](https://doi.org/10.1002/ccd.27514)
 15. Goitein O, Fink N, Hay I, Di Segni E, Guetta V, Goitein D, et al. Cardiac CT Angiography (CCTA) predicts left atrial appendage occluder device size and procedure outcome. *Int J Cardiovasc Imaging*. 2017;33:739-747. DOI: [10.1007/s10554-016-1050-6](https://doi.org/10.1007/s10554-016-1050-6)
 16. Hell MM, Achenbach S, Yoo IS, Franke J, Blachutzik F, Roether J, et al. 3D printing for sizing left atrial appendage closure device: head-to-head comparison with computed tomography and transoesophageal echocardiography. *EuroIntervention*. 2017;13:1234-1241. DOI: [10.4244/EIJ-D-17-00359](https://doi.org/10.4244/EIJ-D-17-00359)
 17. Liu P, Liu R, Zhang Y, Liu Y, Tang X, Cheng Y. The Value of 3D Printing Models of Left Atrial Appendage Using Real-Time 3D Transesophageal Echocardiographic Data in Left Atrial Appendage Occlusion: Applications toward an Era of Truly Personalized Medicine. *Cardiology*. 2016;135:255-261. DOI: [10.1159/000447444](https://doi.org/10.1159/000447444)
 18. Obasare E, Mainigi SK, Morris DL, Slipczuk L, Goykhman I, Friend E, et al. CT based 3D printing is superior to transesophageal echocardiography for pre-procedure planning in left atrial appendage device closure. *Int J Cardiovasc Imaging*. 2018;34:821-831. DOI: [10.1007/s10554-017-1289-6](https://doi.org/10.1007/s10554-017-1289-6)
 19. Hozawa M, Morino Y, Matsumoto Y, Tanaka R, Nagata K, Kumagai A, et al. 3D-computed tomography to compare the dimensions of the left atrial appendage in patients with normal sinus rhythm and those with paroxysmal atrial fibrillation. *Heart Vessels*. 2018;33:777-785. DOI: [10.1007/s00380-018-1119-3](https://doi.org/10.1007/s00380-018-1119-3)

Cite this article as: Marwan M, Vaillant A, Ammon F, Bittner D, Hell M, Achenbach S. Assessment of the Dynamism of the Left Atrial Appendage Dimensions: A Computer Tomographic Analysis. *Structural Heart Disease*. 2019;5(5):213-220. DOI: <https://doi.org/10.12945/j.shd.2019.035.18>

Transcatheter Trans-aortic Retrograde Approach for the Closure of Perimembranous Ventricular Septal Defects using Cocoon [Amplatzer Duct Occluder I Like] Device – An Initial Experience from a Single Centre

Pankaj Jariwala, MD, DNB, DNB, MNAMS, FICPS, FACC*, Kumar Narayanan, MD, DM, Edla Arjun Padma Kumar, MD, DM

Department of Cardiology, Maxcure-Mediciti Hospitals, Hyderabad, Telangana, India

Abstract

Aims & Objective: Transcatheter ventricular septal defect (VSD) device closure is usually performed using the antegrade approach [1–3]. A few case series of a retrograde technique using the Amplatzer duct occluder (ADO) II device have been reported [4, 5]. We aimed to assess the feasibility and safety of a retrograde closure technique using an ADO I like device, which is used for the closure of patent ductus arteriosus (PDA).

Methods: Between June 2015 and January 2018, eight consecutive, consenting cases with congenital perimembranous VSDs underwent trans-aortic device closure using an ADO I like device in a single tertiary care center.

Results: The median age was 17.1 years (5-32, SD 17.125 years) with 3 males and 5 females. Mean defect size was 6.6 mm (4.5 - 8.6 mm, SD 6.6125), with a median aortic rim of 3.4 mm (2-5, SD 3.4125). Median Qp/Qs and right ventricular systolic pressure was 1.8 (1.6-2.1, SD 1.825) and 41.3 mm Hg (33-50, SD 41.25) respectively. Median fluoroscopy and procedure times were 13.3 (10.6-15.7, SD 13.275) and 23.5 (18.2-27.2, SD 22.722) minutes respectively. The defects were successfully closed with no residual shunt in all 8 patients (100%). There was no

semilunar or atrioventricular valve leaflet entrapment or regurgitation. There were no instances of acute device dislodgement or Atrioventricular (AV) block. Over a median follow up of 18 months, all eight patients remained symptom free with no residual shunt or late complications.

Conclusion: In this initial experience, trans-aortic, retrograde VSD device closure using an ADO I like device appears feasible and safe in patients with perimembranous VSDs which a cost effective alternative to routine use of the ADO II device.

Copyright © 2019 Science International Corp.

Key Words

Ventricular septal defects • Device closure • Duct occluder

Introduction

Transcatheter ventricular septal defect (VSD) device closure is a commonly performed procedure to close perimembranous VSDs (PMVSD), especially those that are moderately restrictive without severe pulmonary artery hypertension. Transcatheter clo-





Figure 1. Cocoon device, which is an Amplatzer duct occluder I [ADO I] like device used for the closure of patent ductus occluder. [Reproduced with permission]

sure is preferred wherever possible in view of shorter hospital stay, easier recovery, cost-effectiveness, and cosmetic reasons.

The procedure is commonly done by an antegrade technique via the right ventricle, using an arterio-venous loop. A trans-aortic retrograde technique using Amplatzer membranous or duct occluder (ADO) II has also been described [1]. Though procedure time and radiation exposure is less with the retrograde technique it has certain limitations. It cannot be used in patients with perimembranous VSDs with aortic rim less than 3 mm [1]. Secondly, the ADO II device is expensive and its routine use, especially in resource-limited settings may not be cost effective. We therefore aimed to assess the feasibility and safety of a retrograde technique for VSD device closure using an indigenously manufactured low cost ADO I like device. We further aimed to demonstrate that this approach could be used irrespective of the adequacy of the aortic rim.

Methods

Patient population

This series included eight consecutive patients with perimembranous VSDs who underwent percutaneous VSD device closure by the trans-aortic retro-

grade approach using an ADO I like device at a single tertiary care center in South India over a three year period (2015-2018). The hospital institutional review board and ethics committee approved the study. All patients gave informed consent. VSD closure was performed as per standard indications in symptomatic patients, with significant shunt as evidenced by standard clinical (mid-diastolic flow murmur), electrocardiographic (left atrial enlargement, left ventricular hypertrophy) or imaging criteria ($Q_p/Q_s > 1.5$ by echocardiography or cardiac catheterization). Perimembranous VSDs with aortic rim less than 5 mm were also included.

Cases that had significant aortic valve prolapse with aortic insufficiency, defect size >10 mm, and severe pulmonary hypertension were excluded. The patients underwent clinical and echocardiographic follow-up one week after the procedure and then once every three months for one year.

Description of technique

Infective endocarditis prophylaxis was administered in all cases. Calculation of VSD diameter and its relation to the aortic valve was determined using trans-thoracic echocardiography (TTE) (Figure 2A & B) only without performing ventriculography. Following femoral arterial access with a 7 French sheath, the defect was crossed from the left ventricle using an exchangeable 0.035-inch angulated floppy hydrophilic guide wire (Radio focus, Terumo cooperation, Tokyo, Japan) through either a Judkins right or Amplatz right diagnostic coronary artery catheter (Medtronic, Minnesota, USA) (Figure 3A). The catheter was then advanced over the wire into either the pulmonary artery (PA) or superior vena cava (SVC). The hydrophilic wire exchanged for an Amplatz extra-stiff soft tip wire (Cook Medical Inc. Bloomington, USA). A 7-8 Fr. delivery sheath along with its dilator which used for the closure of patent ductus arteriosus (PDA), was advanced through the defect into the right ventricle (RV) over the Amplatz stiff wire. The sheath was advanced slowly towards the apex of the RV while withdrawing the dilator and was positioned 3-5 cm beyond the defect (Figure 3B). A device 1 to 2 mm larger than the measured VSD diameter was pre-loaded on a delivery cable and advanced to the tip of the delivery sheath. The entire system was then withdrawn

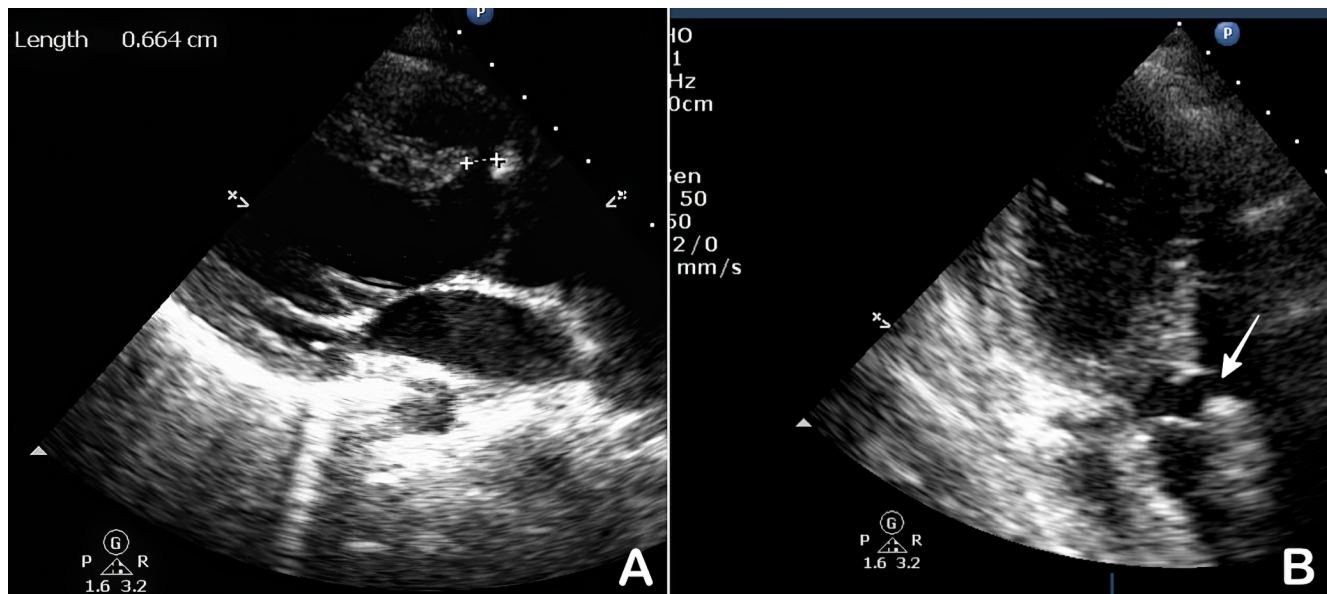


Figure 2. Pre-procedure Trans-thoracic Echocardiography of an illustrated case in Parasternal long axis (*Panel A*) and apical long axis view (*Panel B*) demonstrating a perimembranous ventricular septal defect for the measurement of size of the defect.

back towards the VSD under fluoroscopic and trans-thoracic echocardiographic guidance (*Figure 3C*). The RV disc was exteriorized 1–2 cm distal to the defect while avoiding entrapment of the chordal elements of the tricuspid valve. The whole system was then further withdrawn till the RV disc was firmly seated on the RV aspect of the defect. Keeping it steady, the

sheath alone was then further pulled back to successively deploy the waist and finally the LV disc of the device. Check angiography was performed through the side arm of the delivery sheath by hand injection to confirm device position. TTE was also performed to visualize the placement of the device on the defect, function of the tricuspid, mitral, and aortic valves and

Table 1: Demographic features of the cases, anatomic characteristics of the defects, and data of hemodynamic studies.

Case no	Patient Initials	Age, years	Gender	Height/weight/BMI, Kg/M2	Defect Diameter, mm	Aortic rim, mm	Qp/Qs	RVSP, mmHg
1	BS	11	F	34/140,17.3	5	4	1.8	38
2	PK	5	M	17/108,14.6	5.5	2.5	1.9	45
3	PB	32	M	78/178,24.6	8	3.5	2.0	50
4	YP	25	M	68/170,23.5	8.6	3.8	1.6	35
5	KB	20	F	55/160,21.5	6.7	5	1.8	44
6	PP	9	F	25/128,15.3	4.5	3.6	1.75	37
7	SD	20	F	53/162,20.2	8	2	2.1	48
8	YK	15	F	48/155,20.0	6.6	2.9	1.65	33
Median		17.12		47.25/150.1,19.6	6.6	3.41	1.82	41.25
SD		17.125		47.25/150.125/19.625	6.6125	3.4125	1.825	41.25

BMI: Body mass index; Kg: kilograms; M2: square meter; mm: millimeter; Qp/Qs: Shunt fraction; mmHg: millimeter of Mercury; RVSP: right ventricular systolic pressure; M: male; F: female; SD: Standard Deviation.

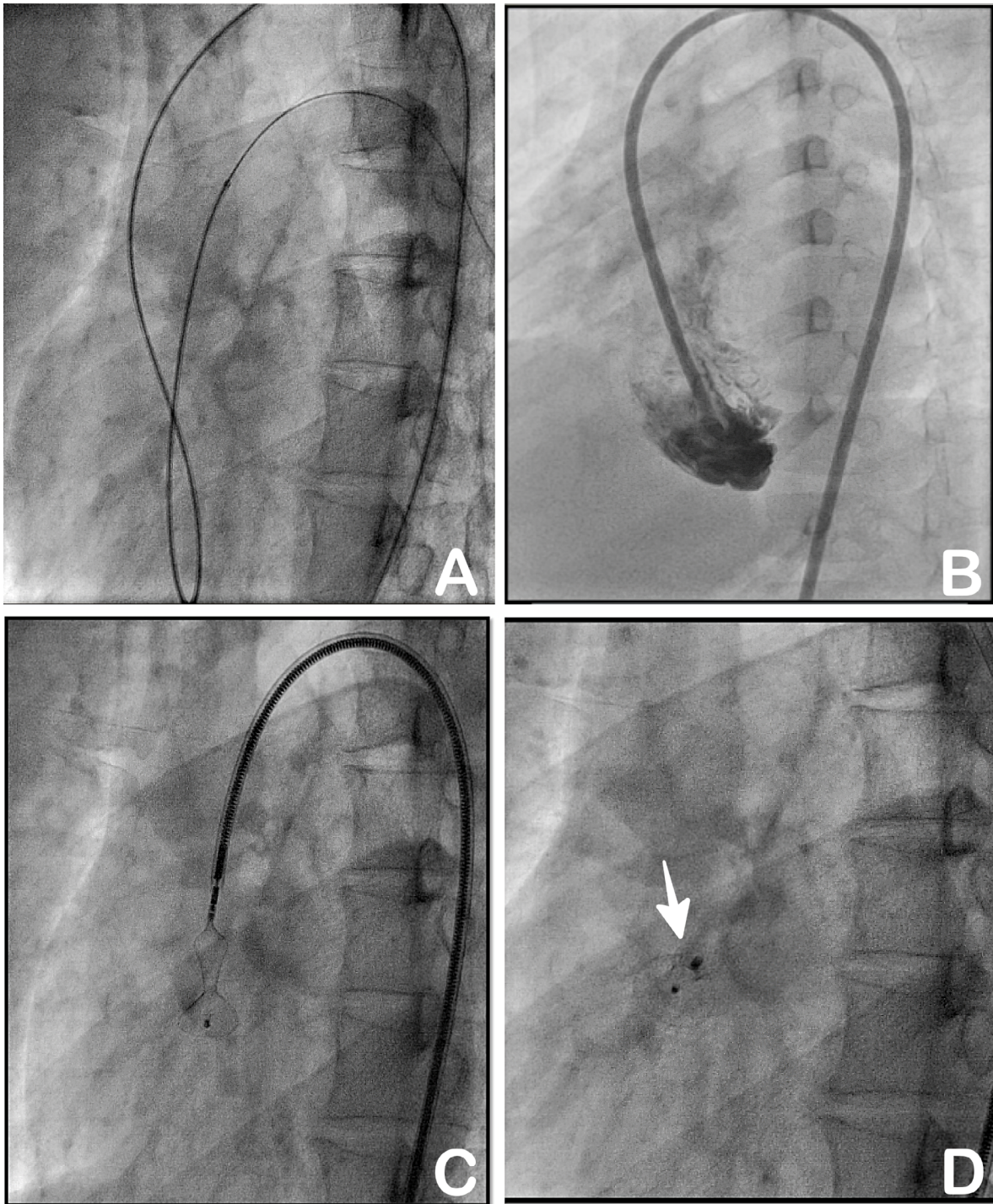


Figure 3. The steps of the procedure (an illustrated case): 0.035-inch angulated floppy hydrophilic guide wire, Terumo from the left ventricle through a Judkins right diagnostic catheter was advanced to the pulmonary artery exchanged with an Amplatz extra-stiff wire. **Panel A.** 7Fr. long delivery sheath of PDA was advanced through the defect into the right ventricle over the rigid wire which was advanced further to the apex of the right ventricle. It was confirmed by hand injection of contrast through the side arm of the delivery sheath. **Panel B.** Complete system was withdrawn with the exteriorized RV disc to be deployed on the right ventricular side and waist of the device across the defect. **Panel C.** The device was released after confirmation of its position across the defect (**Panel D**) by trans-thoracic ecocardiography which also rules out aortic regurgitation.

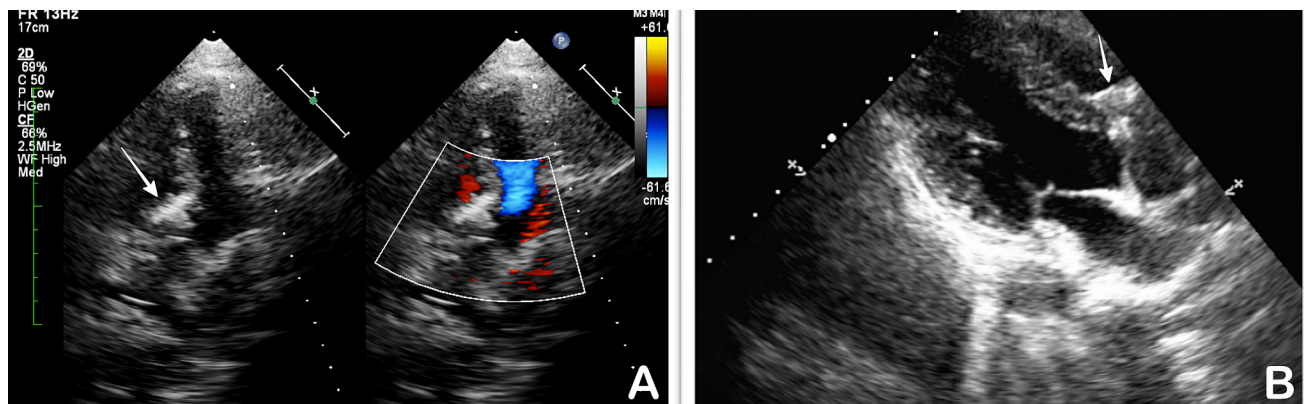


Figure 4. Post-procedure Trans-thoracic Echocardiography (an illustrated case) in four chamber view (*color compare, Panel A*) and parasternal long axis view (*Panel B*) after the procedure which demonstrated the secure, well aligned position of the ADO I like device across the defect without any residual shunt and aortic, mitral or tricuspid regurgitations. The *white solid arrow* showing right ventricular disc and no disc on left ventricular side (*White asterisk*).

any residual shunt prior to finally releasing the device (*Figure 3D*) All patients were administered dual anti-platelet therapy with acetylsalicylic acid 3-5 mg/kg/day and clopidogrel 1-2 mg/Kg/day for the duration of six months post device closure.

Close follow-up was done on 10th day post-discharge using Clinical examination and TTE. (*Figure 4*) Thereafter, patients were followed every 3 months for the period of one year or earlier if patients develop any symptoms in the form of breathlessness, giddiness or syncope. After one year, follow – ups were advised either symptom driven or every 4 to 6 months.

Occluder devices

We used the 'Cocoon' PDA device [manufactured by Vascular Innovations Co. Ltd. Nonthaburi, Thailand & marketed by Vascular Concepts, Bangalore, India] which is very similar to the Amplatzer duct occluder I (ADO I) in terms of design and implantation technique (*Figure 1*).

Results

Between June 2015 and January 2018, eight patients underwent VSD device closure using the technique and device described above. Demographic and clinical characteristics of the cases are summarized in *Table 1*. The median age was 17.1 years (range 5-32 years) with 3 males and 5 females. All patients had perimembranous ventricular septal defects. Mean de-

fect size was 6.6 mm (4.5 - 8.6 mm), with a median aortic rim of 3.4 mm (range 2-5 mm). Aortic rims were < 5 mm in all cases except one. Median Qp/Qs and right ventricular systolic pressure were 1.8 (range: 1.6–2.1) and 41.3 mm Hg (range: 33– 50 mm Hg) respectively.

All patients underwent successful VSD device closure using the retrograde approach. The procedural details are presented in *Table 2*. Median fluoroscopy and procedure times were 13.3 (10.6-15.7) and 23.5 (18.2-27.2) minutes respectively. Device sizes ranged from 4/6 to 10/12 mm and 10/12 mm was the maximum size used in this series. One patient had minimal residual shunt and the rest had no residual shunt acutely after device deployment. There was no impingement on either the tricuspid or aortic valves from the device with no instances of valvular regurgitation. Additionally no patient developed hemolytic anemia or jaundice in the post procedure period.

All Patients were discharged 24 hours after the procedure. No acute device dislodgements or AV block were encountered. No other acute complications occurred in the immediate post procedural period and all patients made an uneventful recovery.

Patients were followed for a median of 18 (12 - 28) months during which all stayed asymptomatic with good effort tolerance. There was no residual shunt or late dislodgement of the device by echocardiography in any case. No patient developed delayed conduction system disturbance or AV block.

Table 2: Procedural details of Trans-aortic retrograde VSD closure using ADO I like device.

Case no	Occluder size, mm	Delivery system, Fr	Residual shunt	Fluoroscopy time, min.	Procedure time, min.
1	6/8	7	No	15.6	25.6
2	6/8	7	No	15.7	27.2
3	10/12	8	No	13.2	25.0
4	10/12	8	Minimal	14.4	24.7
5	8/10	7	No	11.1	19.4
6	4/6	7	No	12.2	18.2
7	10/12	8	No	13.4	22.3
8	6/8	7	No	10.6	18.6
Median				13.3	23.5
SD				13.275	22.722

mm: millimeter; Fr: French size; min: Minutes; SD: Standard Deviation

Discussion

To the best of our knowledge, this is the first reported case series in literature using a combination of retrograde VSD device closure technique and ADO I like device. Though the retrograde approach has been described before using the ADO II device [1–3], there are some limitations in cases with aortic rim less than 5 mm and more procedure time and radiation exposure. The ADO II device is also relatively expensive to use in resource limited contexts such as the Indian setting. Koneti et al. reported the fluoroscopy time of 14 minutes in their series where trans-arterial retrograde technique was done using an ADO II device. [4] In our series, fluoroscopy time was 13.3 minutes. As our experience grew, there was further reduction of fluoroscopy time from 15.7 to 10.6 minutes.

In this series, we used an ADO I like device - 'Coocoon Device' [manufactured by Vascular Innovations Co. Ltd. Nonthaburi, Thailand & marketed by Vascular Concepts, Bangalore, India] for the first time using a trans-aortic retrograde technique. We were able to use this device in all cases irrespective of aortic rim size. Another advantage of using ADO I like device is that it has a low profile with small retention disc on the right ventricular side and no disc on the left ventricular side which lowers the risk of encroachment on vital cardiac structures. We also used 7/8 Fr

PDA delivery systems, which helped in achieving better stability for delivery of device without any twist or kink across the interventricular septum. Koneti et al., on the other hand, used the right coronary guide catheter for the delivery of retrograde devices. They encountered tortuosity of the catheter while across the septum which was overcome by using an extra support coronary guide wire (buddy wire) [1].

Porstmann et al. did the first trans-catheter closure of Patent Ductus Arteriosus (PDA) in 1967. Later, Lock et al. reported transcatheter closure of VSD using 'Rashkind double umbrella' device in 1988 [5]. After the introduction of the Amplatzer device in 1999, the closure of muscular VSDs using the Amplatzer muscular VSD occluder (MVSDO) was published in 2002. Though transcatheter closure of muscular VSDs, was a better option than surgical closure, significant incidence of atrioventricular block varying from to 3-20% was seen [6]. Despite the development of the dedicated Amplatzer Perimembranous VSD Occluder (PMVSDO) for the closure of perimembranous VSDs, a occurrence of AVB was a concern [7, 8]. The tranvenous antegrade technique had more radiation exposure and cumbersome procedure. The trans-arterial retrograde technique, initially using the Amplatzer symmetrical muscular VSD device [9, 10] and subsequently the ADO II device to minimize the risk of atrioventricular block (AVB) and tricuspid valve en-

trapment with possible tricuspid regurgitation during follow-up, got more attention [2, 4]. The advantage of this approach is that it is also useful in patients with venous anomalies, such as interrupted inferior vena cava [11]. It has been reported that the trans-aortic approach causes a lower incidence of AVB than the antegrade approach [9, 12].

ADO I or its chinese counterparts were used in a few case reports by antegrade approach for the closure of residual post-surgical VSDs [13, 14] and for the closure of multi-perforated perimembranous VSD with aneurysm [15]. Recently, Nguyen et al. published a multicenter case series of antegrade transvenous closure of PMVSD using ADO I with 95% success rate and with complications in 1.7% of cases. They had embolization of device in 1% of cases and AVB in 0.7% of cases [16].

The risk of embolization is inherent complication of any device closure but in our case, the non-presence of disc on the LV side doesnot increase it further. Basically, device sits there as it fits snugly and the LV pressure cannot push the device as the LV contracts circumferentially in systole by rotation and torsion [17]. In our small case series, there were no embolization and also no evidence of tricuspid regurgitation. One case had minimal residual shunt which resolved completely at the 1-month follow-up.

Study limitations

Our study had a small number of cases, and should be considered an initial feasibility study. More long-

term data with larger number of patients will be needed to draw more definitive conclusions. In this initial series, we did not attempt to close larger defect sizes, patients < 3 years of age or those with severe reversible pulmonary artery hypertension; hence our findings may not be applicable to these subsets. However the data from this early study appears promising and should prompt further evaluation in a wider spectrum of patients.

Conclusion

In this initial experience, retrograde trans-arterial closure of VSD using an ADO-I like device appears feasible and relatively more cost-effective. It can help further reduce radiation exposure and can be potentially applied in all cases even with deficient aortic rim. Further studies are required to document its efficacy, safety and long-term results in a larger number of patients.

Conflict of Interest

The authors have no conflict of interest relevant to this publication.

Comment on this Article or Ask a Question

References

- Koneti NR, Sreeram N, Penumatsa RR, Arramraj SK, Karunakar V, Trieschmann U. Transcatheter Retrograde Closure of Perimembranous Ventricular Septal Defects in Children With the Amplatzer Duct Occluder II Device. *J Am Coll Cardiol*. 2012;60:2421-2422. DOI: [10.1016/j.jacc.2012.08.1004](https://doi.org/10.1016/j.jacc.2012.08.1004)
- Suligoj B, Cernic N, Zorc M, Noc M, Kar S. Retrograde transcatheter closure of ventricular septal defect with Amplatzer Duct Occluder II. *Postep w Kardiologii Interwencyjnej*. 2016;12:177-178. DOI: [10.5114/aic.2016.59371](https://doi.org/10.5114/aic.2016.59371)
- Pekel N, Ercan E, Özpeli ME, Özyurtlu F, Yılmaz A, Topaloğlu C, et al. Directly ventricular septal defect closure without using arteriovenous wire loop: Our adult case series using transarterial retrograde approach. *Anatol J Cardiol*. 2017;461-468. DOI: [10.14744/AnatolJCardiol.2017.7507](https://doi.org/10.14744/AnatolJCardiol.2017.7507)
- Koneti NR, Penumatsa RR, Kanchi V, Arramraj SK, S J, Bhupathiraju S. Retrograde transcatheter closure of ventricular septal defects in children using the Amplatzer Duct Occluder II. *Catheter Cardiovasc Interv*. 2011;77:252-259. DOI: [10.1002/ccd.22675](https://doi.org/10.1002/ccd.22675)
- Lock JE, Block PC, McKay RG, Baim DS, Keane JF. Transcatheter closure of ventricular septal defects. *Circulation* 1988;78:361-368. DOI: [10.1161/01.CIR.78.2.361](https://doi.org/10.1161/01.CIR.78.2.361)
- Thanopoulos BD, Tsaousis GS, Konstadopoulou GN, Zarayelyan AG. Transcatheter closure of muscular ventricular septal defects with the Amplatzer ventricular septal defect occluder: Initial clinical applications in children. *J Am Coll Cardiol*. 1999;33:1395-1399. DOI: [10.1016/S0735-1097\(99\)00011-X](https://doi.org/10.1016/S0735-1097(99)00011-X)
- Szkutnik M, Kusa J, Białkowski J. Percutaneous closure of perimembranous ventricular septal defects with Amplatzer occluders—a single centre experience. *Kardiologia Pol*. 2008;66:941-949. PMID: [18924021](https://pubmed.ncbi.nlm.nih.gov/18924021/)
- Carminati M, Butera G, Chessa M, Drago M, Negura D, Piazza L. Transcatheter closure of congenital ventricular septal defect with Amplatzer septal occluders. *Am J Cardiol*. 2005;96:52L-58L. DOI: [10.1016/j.amjcard.2005.09.068](https://doi.org/10.1016/j.amjcard.2005.09.068)
- Muthusamy K. Retrograde closure of perimembranous ventricular septal defect us-

- ing muscular ventricular septal occluder: a single-center experience of a novel technique. *Pediatr Cardiol.* 2015;36:106-110. DOI: [10.1007/s00246-014-0971-x](https://doi.org/10.1007/s00246-014-0971-x)
10. Szkutnik M, Qureshi SA, Kusa J, Rosenthal E, Bialkowski J. Use of the Amplatzer muscular ventricular septal defect occluder for closure of perimembranous ventricular septal defects. *Heart.* 2007;93:355-358. DOI: [10.1136/hrt.2006.096321](https://doi.org/10.1136/hrt.2006.096321)
 11. El-sisi A, Ali S. Retrograde Percutaneous Closure of a Perimembranous Ventricular Septal Defect with an Occluder Device in a Child with Interrupted Inferior Vena Cava. *J Struct Hear Dis.* 2017;3:111-114. DOI: [10.12945/j.jshd.2017.014.16](https://doi.org/10.12945/j.jshd.2017.014.16)
 12. Goy J-J, Ruchat P, Stolt V, Schlueter L, Berger A. Percutaneous closure of ventricular septal defect following aortic valve replacement. *Kardiovaskulare Medizin.* 2014;17:266-268. DOI: [10.4414/cvm.2014.00270](https://doi.org/10.4414/cvm.2014.00270)
 13. Djer MM, Idris NS, Alwi I, Wijaya IP. Transcatheter closure of post-operative residual ventricular septal defect using a patent ductus arteriosus closure device in an adult: a case report. *Acta Med Indones.* 2014;46:233-237. PMID: [25348186](https://pubmed.ncbi.nlm.nih.gov/25348186/)
 14. Vaidyanathan B, Kannan BR, Kumar RK. Device closure of residual ventricular septal defect after repair of tetralogy of Fallot using the amplatzer duct occluder. *Indian Heart J.* 2005;57:164-166. PMID: [16013358](https://pubmed.ncbi.nlm.nih.gov/16013358/)
 15. Wierzyk A, Szkutnik M, Fiszer R, Banaszak P, Pawlak S, Biakowski J. Transcatheter closure of ventricular septal defects with nitinol wire occluders of type patent ductus arteriosus. *Postep w Kardiol Interwencyjnej.* 2014;10:21-25. DOI: [10.5114/pwki.2014.41462](https://doi.org/10.5114/pwki.2014.41462)
 16. Nguyen HL, Phan QT, Doan DD, Dinh LH, Tran HB, Sharmin S, et al. Percutaneous closure of perimembranous ventricular septal defect using patent ductus arteriosus occluders. *PLoS One.* 2018;13:e0206535. DOI: [10.1371/journal.pone.0206535](https://doi.org/10.1371/journal.pone.0206535)
 17. Nakatani S. Left Ventricular Rotation and Twist: Why Should We Learn? *J Cardiovasc Ultrasound.* 2011;19:1-6. DOI: [10.4250/jcu.2011.19.1.1](https://doi.org/10.4250/jcu.2011.19.1.1)

Cite this article as: Jariwala P, Narayanan K, Kumar EAP. Transcatheter Trans-aortic Retrograde Approach for the Closure of Perimembranous Ventricular Septal Defects using Cocoon [Amplatzer Duct occluder I Like] device – An Initial Experience from a Single Centre. *Structural Heart Disease.* 2019;5(5):221-228. DOI: <https://doi.org/10.12945/j.jshd.2019.002.19>

Entrapped Stent Delivery Catheter Shaft After High Risk TAVI: Retrieval & Lessons Learned

Safwan Kassas, MD^{1*}, Peter Fattal, MD², Manoj Sharma, MD³

¹ Structural cardiology, Michigan Cardiovascular Institute, Ascension ST Mary's of Michigan, Saginaw, MI, USA

² Cardiac Imaging, Michigan Cardiovascular Institute, Ascension ST Mary's of Michigan, Saginaw, MI, United States

³ Cardiology Division, Covenant Health Care, Saginaw, MI, United States

Abstract

This case report will discuss a first reported complication of very high coronary occlusion risk related to valve-in-valve (VIV) balloon expandable transcatheter aortic valve replacement (TAVR). As a protective measure, an undeployed coronary stent was placed in the left anterior descending (LAD) artery. During the transcatheter heart valve (THV) deployment, the shaft of the left coronary stent catheter was firmly entrapped between the surgical valve posts and the balloon expandable TAVR frame. This prohibited the retrieval and movement of the coronary stent catheter. There were two subsequent ruptures and detachments of the coronary stent catheter while attempting to retrieve the catheter. This report will provide measures to help avoid this entrapment using VIV/balloon expandable TAVR procedures. Steps taken to successfully manage this complication will be discussed.

Copyright © 2019 Science International Corp.

Key Words

Aortic stenosis • Retrieval of foreign body • Coronary occlusion

Introduction

Transcatheter aortic valve replacement for a deteriorating surgical valve in the aortic position is an approved therapy for both the self-expanding Medtronic and the balloon expandable EDWARDS valves. Coronary occlusion is a recognized complication of the TAVR procedure with a slightly higher incidence in the VIV procedures (as cited in Hamid et al., 2015). One of the protective strategies in high coronary occlusion risk TAVR is to place a coronary an undeployed stent in the coronary artery. If coronary occlusion complication occurs, the stent catheter can be pulled back and the left main or right coronary artery (RCA) ostium can be stented. The stent is extended out to reestablish coronary flow. This bail out strategy seems simple and catastrophic complications can take place, as in this case being reported.

Methods

A 63-year-old female patient with the following risk factors: hypertension, type II diabetes mellitus, dyslipidemia, and age. This patient does have a nor-



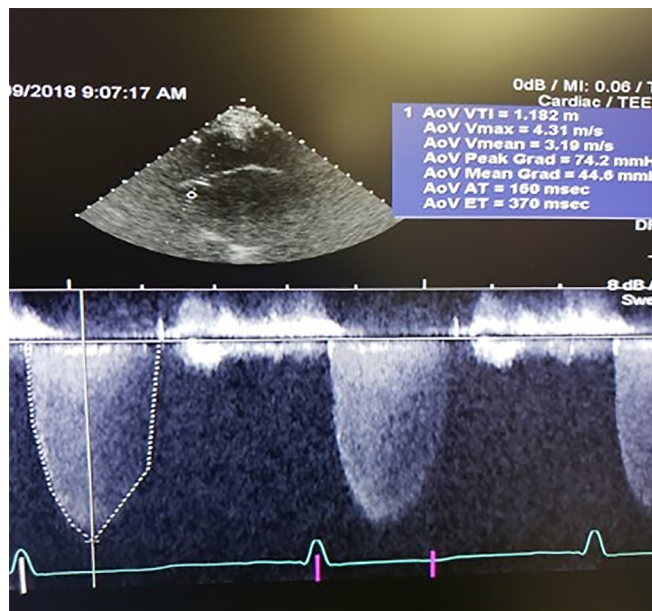


Figure 1. Mean gradient across the bioprosthetic aortic valve of 44 mm Hg indicating severe stenotic process

mal left ventricular ejection fraction (EF) with atrial fibrillation and history of moderate mitral and tricuspid valve regurgitation. This patient has prior cardiac

history of coronary artery disease (CAD) with a LAD stent placed in 2013. In 2011, a 25 mm Carpentier-Edwards Magna pericardial valve was used as an aortic valve replacement. Other past medical history includes: severe chronic obstructive pulmonary disease (COPD) with FEV1 of 0.7 L at 40% predicted, significant renal insufficiency with creatine around 2.0 mg/dL, glomerular filtration rate (GFR) of 32 mL/minute and gastrointestinal bleed with baseline hemoglobin between 8.0 and 9.0 g/dL.

This patient complained of exertional dyspnea with frequent hospital admissions due to congestive heart failure. This was associated with progressive stenotic process in the aortic valve prosthesis with the last mean gradient across the aortic valve prosthesis noted at 44 mmHg (Figure 1). A patient prosthesis mismatch was ruled out due to the mean gradient of 6 mmHg a year post-operatively.

The heart valve team met with this patient to discuss the option of redoing the surgical aortic valve replacement or the transcatheter valve implantation. This case was risk stratified by two cardiac surgeons as a high surgical risk due the calculated STS score of

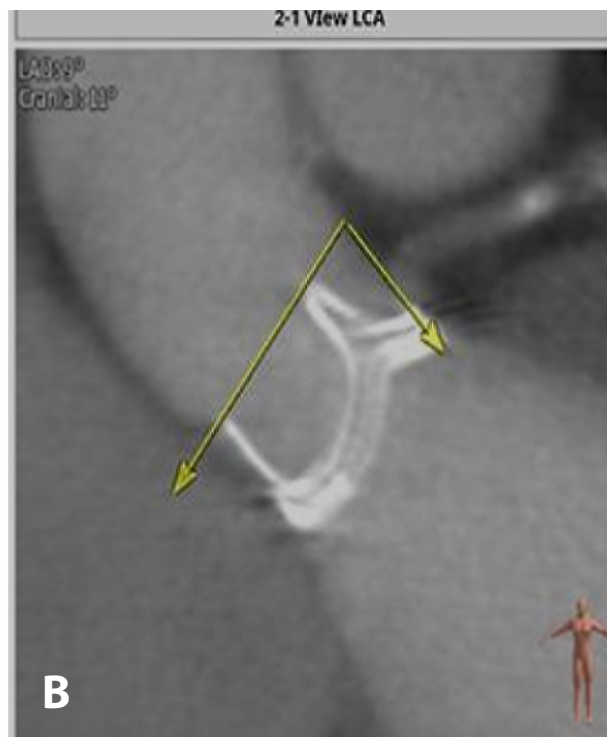
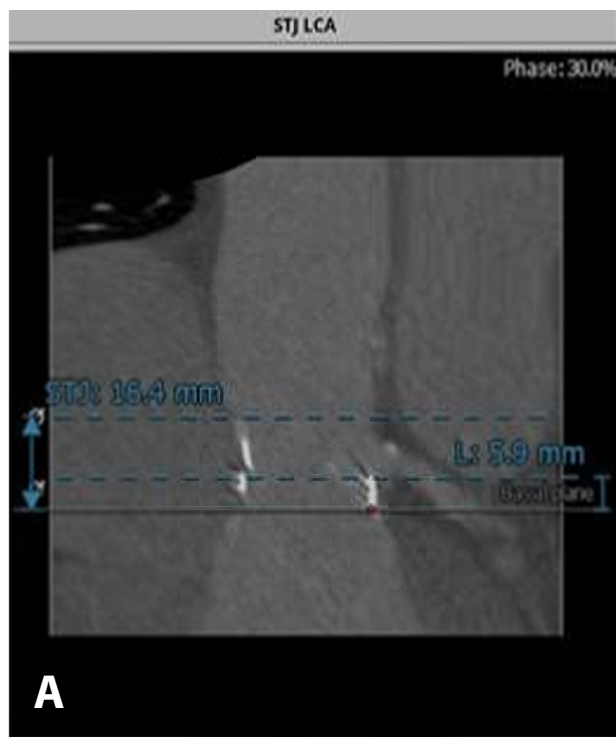


Figure 2. High coronary occlusion risk. *Panel A.* Left main coronary ostial height 5.9 mm. *Panel B.* Surgical frame posts 17 mm slightly higher than STJ 16.7 mm.

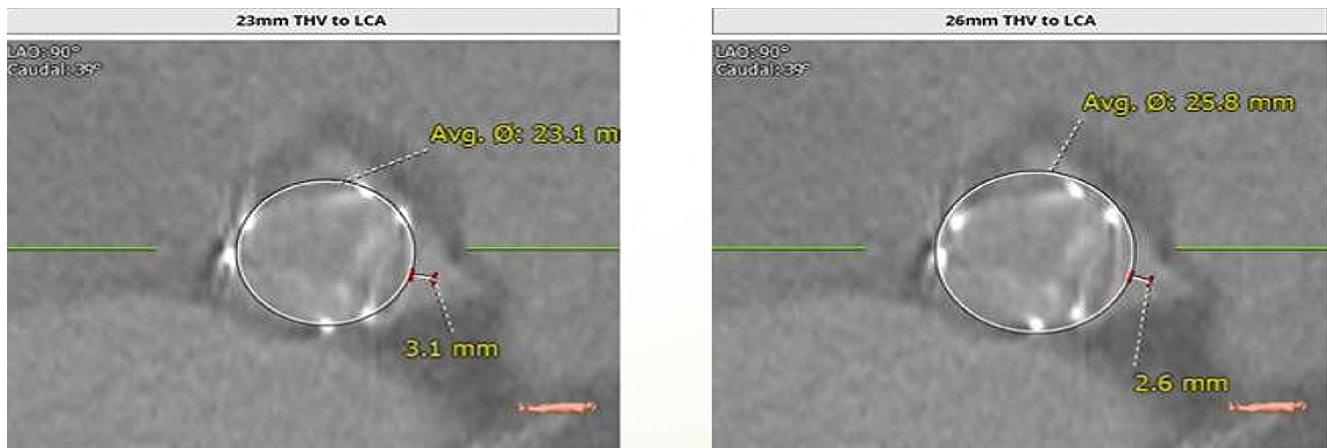


Figure 3. High coronary occlusion risk: Virtual THV coronary distance 3.1 mm for Edwards 23 mm S3 valve and 2.6 mm for Edwards 26 mm valve.

9.6. Another challenge was possibility of the patient declining to undergo redo cardiac surgery. The patient was evaluated for the transcatheter approach. A computed tomography (CT) scan was performed to evaluate the patient's suitability for the VIV procedure and evaluate procedural risks, including coronary occlusion (as cited in Dvir et al., 2015).

The manufacturer profile for the patient's 25 mm Carpentier-Edwards Magna pericardial valve provides a true diameter of 23 mm and posts elevation of 17 mm. The true identifier for the patient's aortic valve prosthesis as measured by CT scan was 21.7 mm by 23.9 mm with an average of 22.8 mm. The sinotubular junction height was 16.4 mm, which was slightly lower than the surgical valve posts. The average diameter was 28.4 mm. The left main coronary ostial height was low at 5.9 mm and the right coronary ostial height was also low at 8.5 mm (Figure 2).

Both the VIV application and the CT evaluation suggested a 26 mm expandable Edwards SAPIEN 3 balloon and transcatheter valve or a 26 mm self-expanding CoreValve. These are the two valves available in the United States.

There is concern about the future difficulty accessing the low coronary arteries with very low ostial height in this patient. The sinus of Valsalva is narrow, while the sinotubular junction height is both low and narrow as compared to the surgical posts height. This made the balloon expandable EDWARDS SAPIEN 3 valve more desirable. However, the patient was at very high risk for both left main and right coronary

artery occlusions (as cited in Dvir et al., 2015). High risk criteria in this case includes: first, the VTC distance (virtual THV to coronary distance), as the virtual THV ring to the left main coronary ostia. The distance was 2.6 mm for a 26 mm EDWARDS SAPIEN3 valve and a 3.1 mm for a 23 mm SAPIEN3 valve (Figure 1). Second, a slightly tilted surgical prosthesis compared to the aortic root long axis. Third, the surgical frame posts are higher than the sinotubular junction at 17 mm versus 16.4 mm. Fourth, a very low coronary ostial height (Figure 3). Fifth, very small sinuses and stenotic valve pathology (Figure 3).

Coronary occlusion risk was discussed with the patient and surgical options were readdressed. However, the patient again declined the redo high risk surgical approach. The patient was offered a transfer to an institution. This institution is capable of splitting the aortic valve surgical prosthesis leaflets to reduce the risk of coronary occlusion (BASILICA procedure) (as cited in Khan et al., 2018). This option was declined due to family circumstances related to travel. This resulted in the patient consenting to the high risk coronary occlusion valve-in-valve TAVR. The following strategies were planned to perform this high coronary occlusion risk valve-in-valve TAVR case. Strategy one is undersizing by using a smaller THV valve at 23 mm rather than 26 mm. Strategy two is using a slightly lower deployment. Strategy three is placing coronary stents in the mid LAD and mid RCA prophylactically as a bail out option if coronary occlusion or compromised flow occurs.

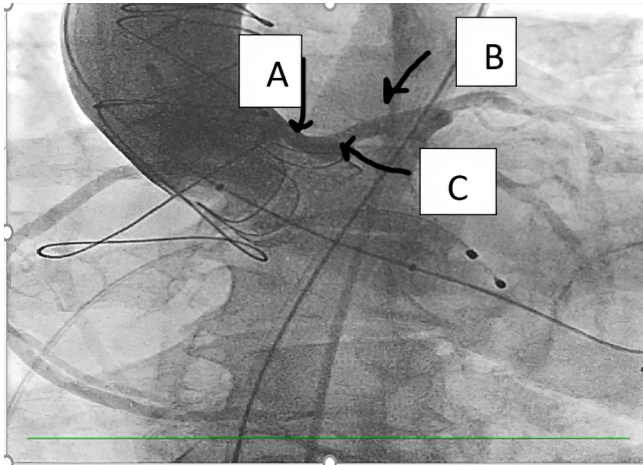


Figure 4. High coronary occlusion risk: Angiographically observed short VTC distance between left main ostium and surgical post. (A) Surgical frame post, (B) Left main artery, (C) Short left VTC distance.

The first strategy was selected. The plan was to use a 23 mm EDWARDS SAPIEN 3 balloon expandable valve instead of the 26 mm valve as suggested by the VIV application and CT analysis. Subsequently, this decision was selected due to the slightly longer VTC distance with a 23 mm valve to lower risk of coronary occlusion. Therefore, a 3.1 mm VTC distance was used versus the 2.6 mm. Doing this created less lateral displacement of the surgical posts with a smaller diameter THV valve. A shorter frame height valve of 23 mm was used instead of the 26 mm SAPIEN 3 valve. The sinotubular junction height in this patient is 16.4 mm, which is why the slightly shorter surgical frame post of 17 mm was selected. This would hypothetically cause less interaction of the surgical posts with the sinotubular junction having a shorter THV frame.

Slightly lower deployment was planned to minimize any potential interaction between the laterally displaced surgical posts and the sinotubular junction because of deployment of the THV valve. The left 2:1, right 2:1 and 1:1:1 fluoroscopic angles were identified and angiographic images were obtained. While using the XB 3.5 and JR4 guide catheters, coronary stents were placed in the mid LAD and mid RCA. There was a high likelihood a left main stent would need to be deployed to create a chimney path next to the THV stent frame. Aortic root angiography during a 23 mm balloon inflation in the left 2:1 angulation and the

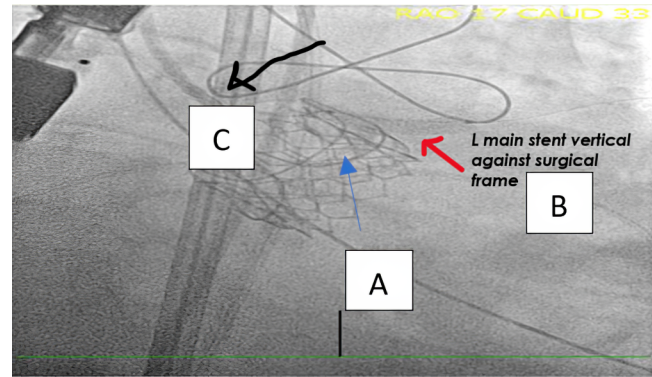


Figure 5. Coronary stent in a vertical trajectory against surgical aortic prosthesis with the stent balloon can not be withdrawn back due to catheter entrapment. (A) THV, surgical prosthesis frames. (B) Left main stent in a vertical trajectory against surgical bioprosthesis with deflated balloon entrapped inside the stent. (C) XB 3.5 guide catheter.

right 2:1 angulation confirmed the high coronary occlusion risk. Thrombolysis in myocardial infarction (TIMI) 3 flow was still maintained in both the left main and RCA during balloon inflation (Figure 4).

The 23 mm EDWARDS SAPIEN 3 valve was deployed in the left 2:1 view to evaluate the interaction between the left main ostium and the surgical valve prosthesis during the THV valve deployment. Towards the end of the THV inflation period an interaction took place between the left coronary stent catheter shaft and the surgical posts/THV frame. Angiography post THV deployment showed the patient continued to have TIMI 3 flow in both the left and right coronary arteries. The wire and stent in the RCA were removed since there was no concern about RCA flow. However, due to the very short distance between the left main ostium and the surgical posts, deployment of the left coronary stent in and out of the left main coronary artery was performed. This created a vertical chimney appearance with a stented path extending to the level of the sinotubular junction. Easy future access could now be obtained if needed to the very low left main coronary artery, which had shallow sinuses and a short VTC distance of 3.1 mm.

Significant resistance was encountered while attempting to pull the stent catheter back from the parked mid LAD segment. While positioning the stent at the left main level, the stent catheter shaft was en-

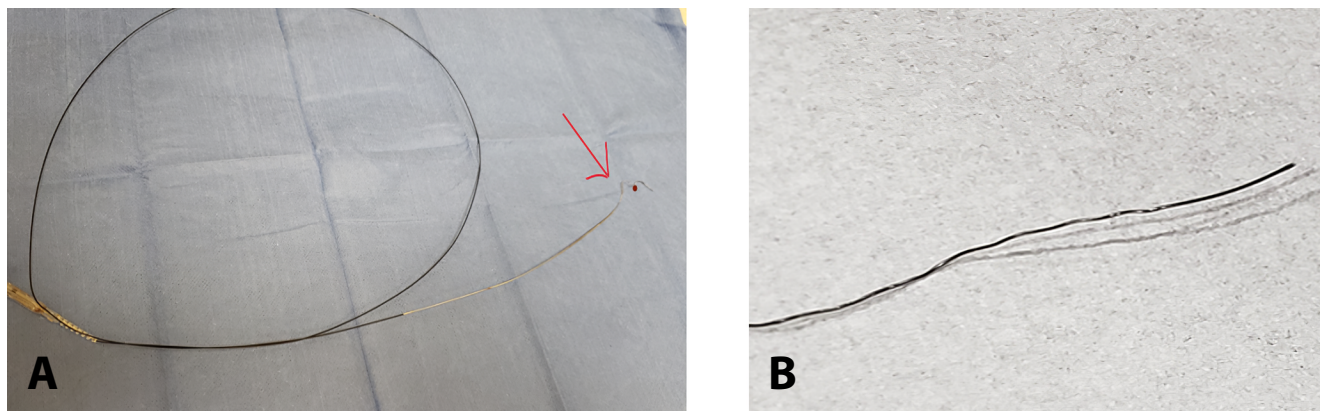


Figure 6. *Panel A.* First rupture of stent catheter shaft at monorail point. *Panel B.* Second rupture of catheter shaft because of snaring.

trapped firmly between the surgical valve posts and the EDWARDS frame. This prohibited the ability to retrieve the catheter. The stent was retrieved while using a mechanical and forceful pull where the coronary stent struts were in contact with the surgical valve/THV frames. No further adjustment forward or backwards was feasible. Therefore, the chimney path that with the intent to be created was unable to be retrieved by the stent catheter. The only available option to proceed was to deploy the left coronary stent in an undesirable position. The stent was partially in the left main artery and extended out, contacting in a vertical trajectory to the surgical/THV frames (Figure 5).

The plan was to be able to drag the stent balloon from its entrapped course between the surgical posts and the SAPIEN 3 frame and remove from the body. The left main coronary artery was rewired through the struts of the existing stent. Balloon dilatation of the left main stent strut was then performed. A second stent was deployed, creating a parallel stented path that was initially felt to be necessary. Since the deflated balloon was unable to be retrieved, the winged balloon failed to pass in-between the surgical post and the SAPIEN 3 THV frame. A manual pulling force was applied to facilitate the retrieval of the stent balloon passing in-between the surgical bioprosthesis post and the EDWARDS SAPIEN 3 frame passage. Unfortunately, the balloon catheter shaft ruptured at the monorail port because of the pulling (Figure 6A). The left main stent was deployed in a poor position with an irretrievable deflated winged balloon inside

it, as previously described. The balloon was partially entrapped between the surgical bioprosthesis post and the EDWARDS SAPIEN 3 frame.

As stated above, the ruptured balloon catheter shaft containing a few centimeters of a short segment remained attached to the entrapped balloon. The ruptured balloon catheter shaft extended a few centimeters into the aortic root. A goose neck snare was successfully used to retrieve the remaining proximal piece of the ruptured balloon catheter shaft out of the aortic root. A pulling force was again applied on the snare to facilitate the passage and retrieval of the entrapped balloon in-between the surgical post and the SAPIEN 3 frame. A second rupture occurred just outside of the surgical post and SAPIEN 3 frame, resulting in no movement of the entrapped deflated winged balloon (Figure 6B).

Access was lost to the partially, yet firmly, entrapped balloon inside the left main stent and in-between the surgical frame post and the SAPIEN 3 frame with no wire access. Attempting to wire the left main stent through a superior strut and next to the entrapped balloon was discussed. The strut was dilated and another stent was deployed. This caused crushing of the entrapped balloon between two layers of the left main stent with the second stent extending further out in a vertical chimney fashion. This granted easy access to the left coronary system. Due to various reasons the left main stent was unable to be wired through a superior stent strut. This was due to the long distance between the guide catheter and the low left main coronary stent. The guide catheter

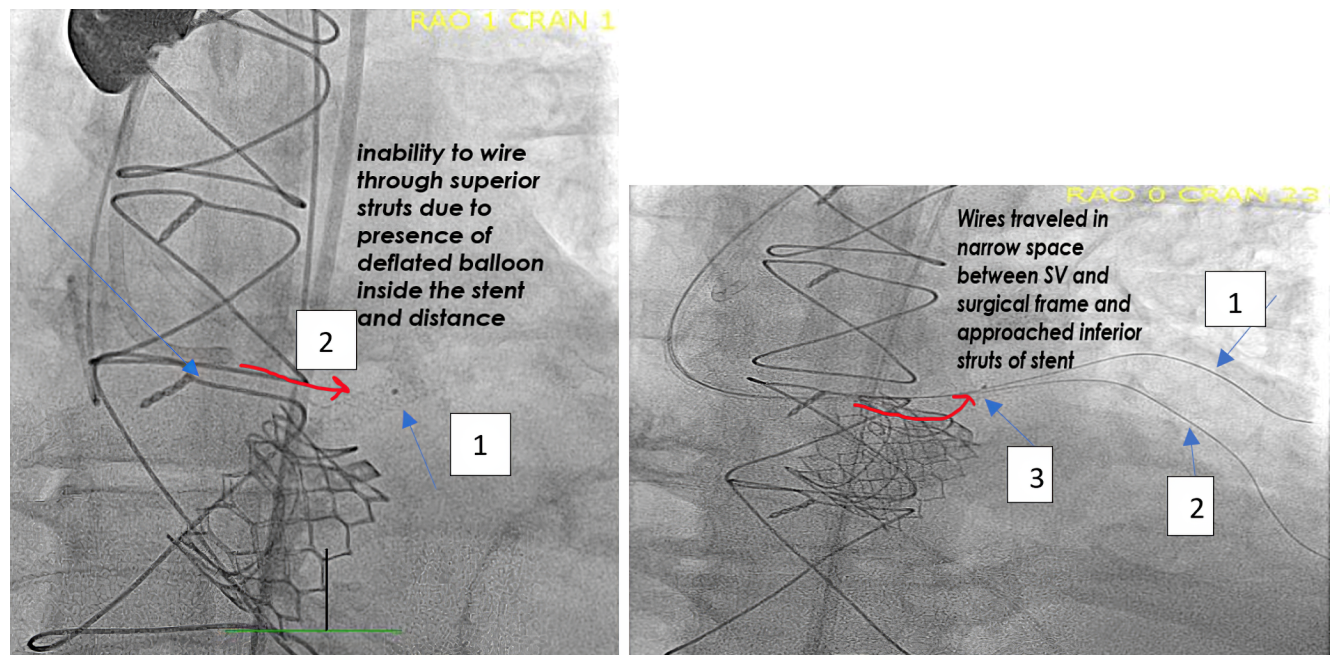


Figure 7. Panel A. Inability to wire through a superior strut due to distance and due to the presence of deflated winged balloon inside the stent. (A1) distal marker of stent balloon (A2) Coronary stent with deflated balloon entrapped inside. Panel B. Successfully wiring the stent through an inferior strut THV. (B1) wire #1 (B2) wire #2 introduced for better support (B3) distal marker of stent balloon.

was unable to advance further due to a narrow sinotubular junction and short VTC distance. Presence of the deflated winged balloon in the lumen of the left main coronary stent prohibited wire advancement (Figure 7A).

The patient remained hemodynamically stable with no electrocardiogram (ECG) changes during the procedure. The left main stent could not be wired from a superior strut with a deflated winged balloon as planned. The left main stent was wired through an inferior strut hoping for a more permissible wire advancement course next to the winged balloon. The hydrophilic wire with two curves at its tip was reshaped. A primary larger curve and a secondary smaller curve was used to advance the wire freely in the narrow distance between the surgical frame and the sinotubular junction. This allowed the hydrophilic wire to go inferior to the stent frame and redirected the wire more superiorly to engage the left main stent from below, through an inferior strut. After significant attempts the wire was advanced and positioned in the apical LAD successfully. The inferior entry strut was dilated with a 2.0 mm balloon and then a 2.5 mm balloon. The same maneuver was used to advance a

second wire for better guide catheter support and to secure access to the left coronary arteries (Figure 7B).

The only option left was to advance a snare catheter distally to the deflated balloon while also attempting to snare the balloon from the distal end in the proximal LAD. An attempt was made to retrieve the deflated balloon backwards, forcing it to make a short U-turn in the proximal lumen of the LAD. This would allow the dilated inferior left main strut to be removed without needing to pass in-between the surgical and the SAPIEN 3 frames. The distal end of the balloon was successfully removed by positioning a snare in the mid LAD and gradually pulling it back to capture the distal nose of the deflated balloon. A forceful pull was again applied, successfully retrieving the deflated balloon outside the left main stent (Figure 8).

The existing left main stent will have a high risk of thrombosis due to its malposition as described above. One way to minimize this risk was to reattempt to wire the left main stent from a superior strut now that the deflated winged balloon was removed and no longer in the way.

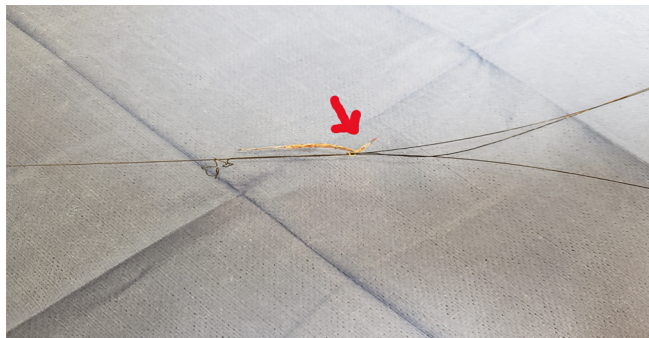


Figure 8. Stent balloon successfully snared and retrieved out of body.

The stent was successfully wired, dilating the superior entry strut. A 4.0 mm by 26 mm long stent extending vertically to the THV/SAPIEN 3 frames was deployed at the level of the sinotubular junction. This was followed by intravascular ultrasound (IVUS) evaluation, which revealed that the stent was undersized. The stent with a 5.0 mm non-compliant balloon was dilated and the procedure ended with a kissing left main. Balloon aortic valvuloplasty was performed using a 5.0 mm coronary balloon and a 24 mm Z-MED balloon. This concluded with an excellent angiographic result (Figure 9). A year later the patient was seen in the office with no recurrent admissions to the

hospital or any cardiac events. Mean gradient across the THV valve was 14 mmHg following one year after the procedure.

Discussion

Transcatheter aortic valve replacement procedures are gaining more popularity with expanding indications. TAVR is already an approved indication for a failing surgical valve. Even though the TAVR procedure has become easier to perform with less complication rates, what remains critical is for the operators to be able to do a thorough analysis of the anatomy. In the case of the VIV procedure, both the structure of the surgical valve and the THV valve must be understood. One must have the ability to predict a complication and have a plan to manage it critically. Unpredicted complications can occur, such as the one reported in this case.

Retrospectively, the images reviewed at the end of the procedure showed an interaction occurred. This occurred during the inflation of the SAPIEN 3 stent valve balloon between the expanding SAPIEN 3 frame and the coronary stent catheter shaft. If noted during the procedure, it could have alerted to the fact that the coronary stent catheter shaft was coursing in-be-

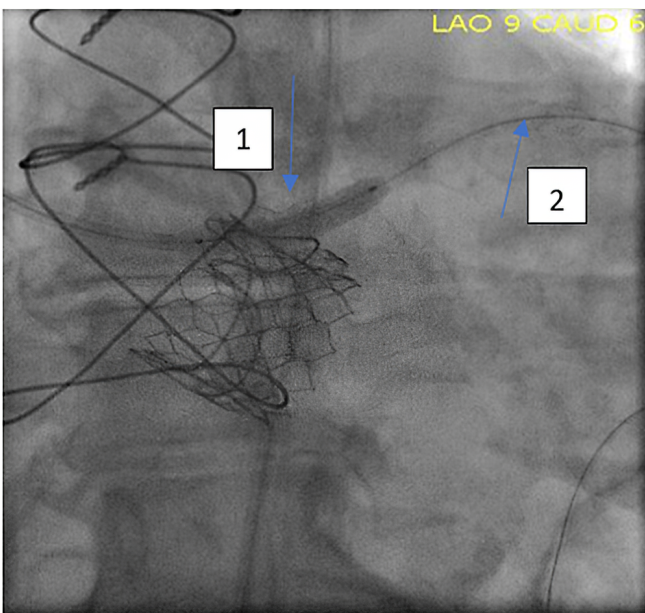
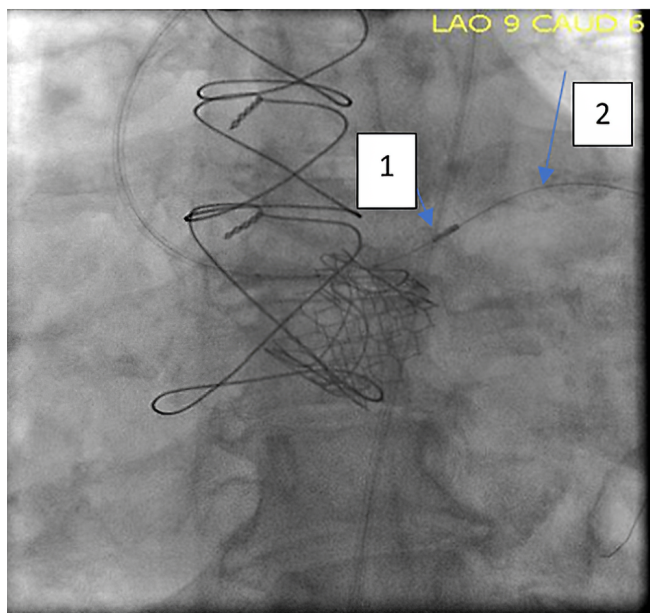


Figure 9. *Panel A.* (A1) IVUS catheter in L main stent. (A2) Wire through superior strut of left main stent. *Panel B.* (B1) Second left main stent creating a chimney path course through a superior strut of the first stent. (B2) Wire through a superior strut of the first left main stent.

tween the surgical frame and the SAPIEN 3 frame. A quick adjustment or pull on the coronary stent catheter shaft could have been made to avoid the entrapment. It is advised to use the following for valve-in-valve TAVR with high occlusion risk where balloon expandable valves are used. Close attention must be paid to the course of guide catheters, wires and coronary stent catheters to avoid entrapment. Monitoring for any interaction between the coronary stent catheter and the expanding THV frame during deployment as any interaction should indicate the coronary stent catheter is coursing in-between the THV and the surgical frames. Careful selection of guide catheters is important, such as using a Judkins left or short tip artery access as previously noted. Using general anesthesia with transesophageal echocardiogram (TEE) guidance allows for the use of smaller sized balloon expandable valves. Slight underfilling and lower deployment is desired as the end result.

Conclusion

Transcatheter aortic valve replacement is gradually becoming the main stream treatment for aortic valve

References

1. Hamid NB, Khaliq OK, Monaghan MJ, Kodali SK, Dvir D, Bapat VN, et al. Transcatheter Valve Implantation in Failed Surgically Inserted Bioprosthesis: Review and Practical Guide to Echocardiographic Imaging in Valve-in-Valve Procedures. *JACC Cardiovasc Imaging*. 2015;8:960-979. DOI: <https://doi.org/10.1016/j.jcmg.2015.01.024>
2. Dvir D, Leipsic J, Blanke P, Ribeiro HB, Kornowski R, Pichard A, et al. Coronary Obstruction in Transcatheter Aortic Valve-in-Valve Implantation Preprocedural Evaluation, Device Selection, Protection, and Treatment. *Circ Cardiovasc Interv*. 2015;8:1. pii: e002079. DOI: <https://doi.org/10.1161/CIRCINTERVENTIONS.114.002079>
3. Khan JM, Dvir D, Greenbaum AB, Babaliaros VC, Rogers T, Aldea G, et al. Transcatheter Laceration of Aortic Leaflets to Prevent Coronary Obstruction During Transcatheter Aortic Valve Replacement: Concept to First-in-Human. *Circ Cardiovasc Interv*. 2018;11:677-689. DOI: <https://doi.org/10.1161/CIRCINTERVENTIONS.114.002079>

stenosis. The skills to perform an interventional procedure are important, but more knowledge and training are indicated to perform the procedure successfully. Operators need to be able to perform careful analysis of the diagnostic data available to them and be able to predict potential risks and complications. Operators also need to be proficient in the various devices commercially available to them. Every operator must be ready to manage complications and be aware that potential unknown difficulties can occur. There is always a first time for everything.

Conflict of Interest

Safwan Kassas received a research grant from Edwards Life Science: Proctor Boston Scientific Inc.

[Comment on this Article or Ask a Question](#)

Cite this article as: Kassas S, Fattal P, Sharma M. Entrapped Stent Delivery Catheter Shaft After High Risk TAVI: Retrieval & Lessons Learned. *Structural Heart Disease*. 2019;5(5):229-236. DOI: <https://doi.org/10.12945/j.jshd.2019.037.18>